AD-A124 488   ADAPTIVE ARRAY PERFORMANCE WITH SPECULAR MULTIPATH(U)   1/1
OHIO STATE UNIV COLUMBUS ELECTROSCIENCE LAB
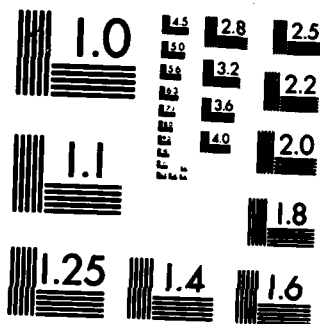K L REINHARD FEB 74 ESL-3576-2 N00019-73-C-0195

UNCLASSIFIED   F/G 20/14   NL
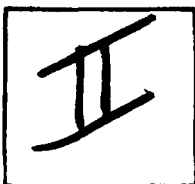
END
DATE
FILMED

DTIC

MICROCOPY RESOLUTION TEST CHART
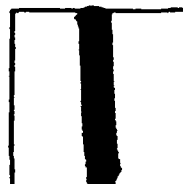
NATIONAL BUREAU OF STANDARDS-1963-A

PHOTOGRAPH THIS SHEET

LEVEL

INVENTORY

Rept. No. ESL-3576-2

DOCUMENT IDENTIFICATION

Contract N00019-73-C-0195   Feb. 74

ACCESSION FOR
NTIS	GRA&I	☒
DTIC	TAB	☐
UNANNOUNCED		☐
JUSTIFICATION		

BY
DISTRIBUTION /
AVAILABILITY CODES
DIST	AVAIL AND/OR SPECIAL
A	

DISTRIBUTION STAMP

DTIC
ELECTE
S FEB 16 1983
D

D

DATE ACCESSIONED
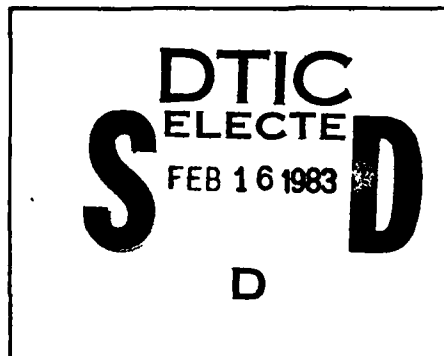
DTIC
COPY
INSPECTED
2

83 02 010 041

DATE RECEIVED IN DTIC

PHOTOGRAPH THIS SHEET AND RETURN TO DTIC-DDA-2

DTIC FORM OCT 79 70A

DOCUMENT PROCESSING SHEET

ADAPTIVE ARRAY PERFORMANCE WITH SPECULAR MULTIPATH
(March 1, 1973 to June 1, 1973)

K. L. Reinhard

The Ohio State University

ElectroScience Laboratory

Department of Electrical Engineering
Columbus, Ohio 43212

QUARTERLY TECHNICAL REPORT 3576-2

February 1974

Contract N00019-73-C-0195

Department of the Navy
Naval Air Systems Command
Washington, D.C. 20360

NOTICES

When Government drawings, specifications, or other data are
used for any purpose other than in connection with a definitely
related Government procurement operation, the United States
Government thereby incurs no responsibility nor any obligation
whatsoever, and the fact that the Government may have formulated,
furnished, or in any way supplied the said drawings, specifications,
or other data, is not to be regarded by implication or otherwise as
in any manner licensing the holder or any other person or corporation,
or conveying any rights or permission to manufacture, use, or sell
any patented invention that may in any way be related thereto.

ADAPTIVE ARRAY PERFORMANCE WITH SPECULAR MULTIPATH
(March 1, 1973 to June 1, 1973)

K. L. Reinhard

QUARTERLY TECHNICAL REPORT 3576-2

February 1974

Contract N00019-73-C-0195

ABSTRACT

This report describes the theoretical performance of an adaptive antenna array in a multipath signal environment. The array response to a coded communication signal comprised of a direct (line-of-sight) component and a specular multipath component is determined for the case in which differential doppler frequency shift between components is negligible compared to the reciprocal time constants of the array processing loops.

Performance analyses are presented which determine the ratio of powers in the direct and multipath signal components at the array output. The fraction of total power at the array output which is usable or beneficial for post-array data demodulation is also calculated. Computer evaluations are presented which illustrate the dependence of these ratios on received signal amplitudes, carrier phases, angle-of-arrival separation, and relative synchronization with a coded reference signal which is locally generated at the receiving array.

TABLE OF CONTENTS

I. INTRODUCTION

Adaptive antenna arrays have been under study for several years. Widrow, et.al.[1] suggested the basic feedback algorithm and did computer simulations of the behavior of such an array. Shor[2] and Applebaum[3] have also studied closely related ideas. Baird and Zahm[4], and Baird, et.al.[5] have investigated the relationships between different performance criteria for adaptive arrays. Early experimental measurements of array performance in a communications environment are described in Riegler and Compton[6]. Compton[7] also discusses the results of extensive measurements with a four-element array in the 200-400 MHz band where the array elements are mounted on an irregular surface. The use of adaptive arrays for clutter rejection in radar has been studied by Brennan and Reed[8]. Berni[9] discusses techniques which employ an adaptive array for angle-of-arrival estimation.

The application of adaptive arrays to interference rejection in coded communication systems has recently been under investigation, both theoretically and experimentally. The behavior of an array with coded signals and a "bootstrap" reference signal generation circuit has been studied with computer simulations by Reinhard[10,11]. Two versions of a coded adaptive array have also been implemented, and the experimental results are described by Huff and Reinhard[12,13], and by Schwegman and Compton[14].

The purpose of this report is to investigate the response of an adaptive array to a coded communication signal when a specular multi-path component is also present in the received signal. Of particular interest is the case where the direct signal and the multipath signal arrive with only a small timing difference (relative to the reciprocal of the signal modulation bandwidth), because this case appears to be potentially the most descriptive to array performance. In this report, we study the array response to such a correlated interfering signal from a theoretical standpoint.

In Section II analytical models of the adaptive array processor and the input signal structure are defined. Certain restrictions in the models which are necessary in order to obtain analytical solutions are discussed. In Section III the performance resulting from these models is analyzed for the case in which the array response has reached steady-state conditions. An expression for the ratio of powers in the signal components at the array output is derived and evaluated numerically in Section III-C. In section III-D the power contained in that portion of the composite array output signal which is correlated with the array reference signal is compared to the power present in the undesired output components. The numerical results presented yield considerable insight into the array behavior.

1

II.   ANALYSIS MODEL

A.   Array Processor Model

The general configuration of an m-element adaptive array is shown in Fig. 1. The receiving electronics for each array element which normally precede the adaptive processor are not shown for simplicity. These electronics include an rf pre-amplifier, a mixer for downconversion to an intermediate frequency (IF), and an IF bandpass amplifier which rejects the upper sideband product of the mixer output.* The array processing consists of separating the composite IF signal plus thermal noise process from each element into quadrature (orthogonal) components, multiplying the quadrature components by real-valued weighting coefficients, and summing the weighted products to form the array output. These operations will be modeled mathematically by an inner product of two vectors: an input vector of complex envelope signals associated with the real IF input signals, and a complex weight vector representing the array weighting functions. The input vector is defined as the column vector

$$(1) \qquad \underline{\tilde{x}}(t) \equiv \begin{bmatrix} \tilde{x}_1(t) \\ \vdots \\ \tilde{x}_k(t) \\ \vdots \\ \tilde{x}_m(t) \end{bmatrix} \qquad ,$$

where the kth component, $\tilde{x}_k(t)$, is the complex envelope (or pre-envelope) of the total signal plus thermal noise process, $x_k(t)$, applied to the quadrature hybrid input from the kth array element. The pre-envelopes are defined at the IF center frequency, f_c, and contain the amplitude and phase modulation of the IF bandpass processes, $x_k(t)$, i.e.,

$$(2) \qquad x_k(t) = \text{Re}\left\{ \tilde{x}_k(t) \cdot \sqrt{2}\, e^{+j\omega_c t} \right\}$$

$$= \sqrt{2}\, |\tilde{x}_k(t)| \cdot \cos[\omega_c t + \text{Arg}\, \tilde{x}_k(t)],$$

$$k = 1, 2, \cdots, m.$$

---

*A common local oscillator signal is applied to the mixer in each element.
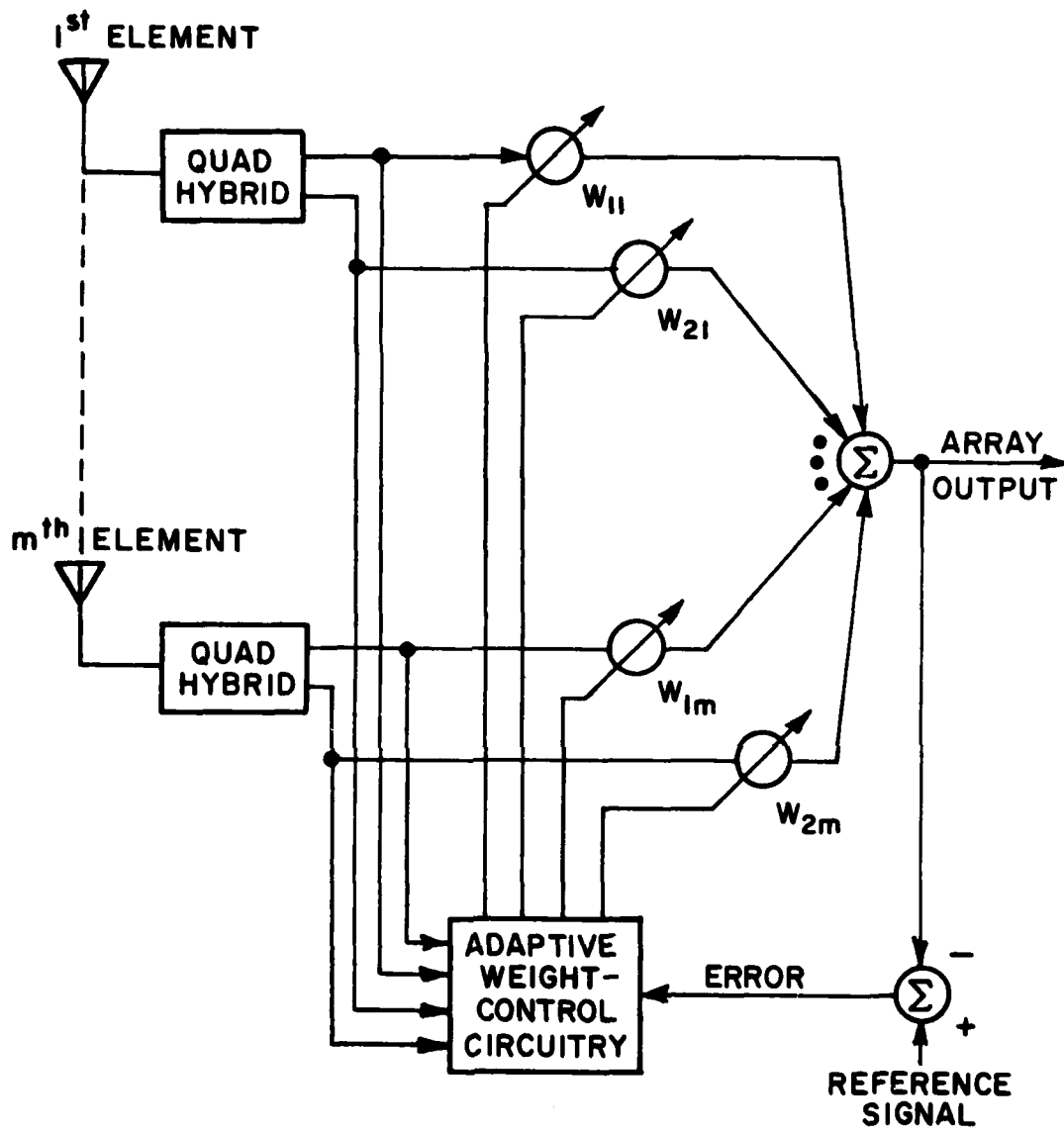
2

Fig. 1. Adaptive array structure.

3

A decomposition of the input vector, Eq. (1), into direct signal, multipath signal, and thermal noise components will be discussed later in Section II-B. The array weight vector is defined as a column vector of complex-valued weighting coefficients,

$$(3) \qquad \underline{w}(t) \equiv \begin{bmatrix} w_1(t) \\ \vdots \\ w_k(t) \\ \vdots \\ w_m(t) \end{bmatrix} \equiv \begin{bmatrix} w_{11}(t) + j\, w_{21}(t) \\ \vdots \\ w_{1k}(t) + j\, w_{2k}(t) \\ \vdots \\ w_{1m}(t) + j\, w_{2m}(t) \end{bmatrix} \quad ,$$

where $w_{1k}(t)$ and $w_{2k}(t)$ are the in-phase and quadrature weights, respectively, associated with the kth array element. As illustrated in Fig. 2, the weighted output process from the kth array element has a pre-envelope given by the product

$$(4)^* \qquad \tilde{\gamma}_k(t) = \tilde{x}_k(t)\, w_{1k}(t) + [-j\, \tilde{x}_k(t)]\, w_{2k}(t)$$

$$= [w_{1k}(t) - j\, w_{2k}(t)]\tilde{x}_k(t) = w_k(t)^\dagger\, \tilde{x}_k(t).$$

The pre-envelope of the array output process is equal to the summation of suboutputs, Eq. (4), over the array element index k, or equivalently by the inner product

$$(5) \qquad \tilde{\gamma}(t) = <\underline{w}(t), \underline{\tilde{x}}(t)> = \underline{w}(t)^\dagger\, \underline{\tilde{x}}(t)$$

$$= \sum_{k=1}^{m} \tilde{\gamma}_k(t) = \sum_{k=1}^{m} w_k(t)^\dagger\, \tilde{x}_k(t).$$

The array is adaptive as a result of weighting coefficient adjustment and control through feedback from the array output. The adaptive weight-control system in Fig. 1 is designed to minimize the difference (error) between the array output and a reference signal. The design is based on a least mean square error (LMSE) performance criterion[1,5,13] and results in weighting coefficient responses governed by the vector differential equation

---

*The symbol $\dagger$ represents the adjoint (complex conjugate transpose) operator. The adjoint of a scalar quantity is simply its conjugate.

4

$$x_k(t) = \mu_k(t)\cos[\omega_c t + \Phi_k(t)]$$

$$\hat{x}_k(t) = \mu_k(t)\sin[\omega_c t + \Phi_k(t)]$$

QUADRATURE HYBRID

(a)

(b)
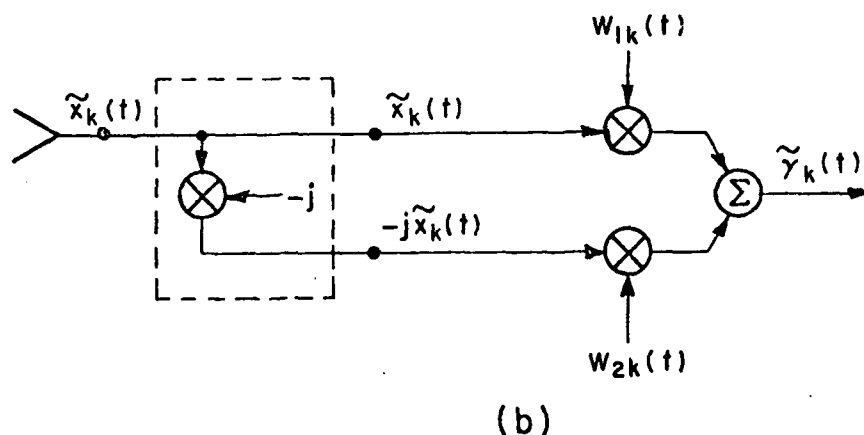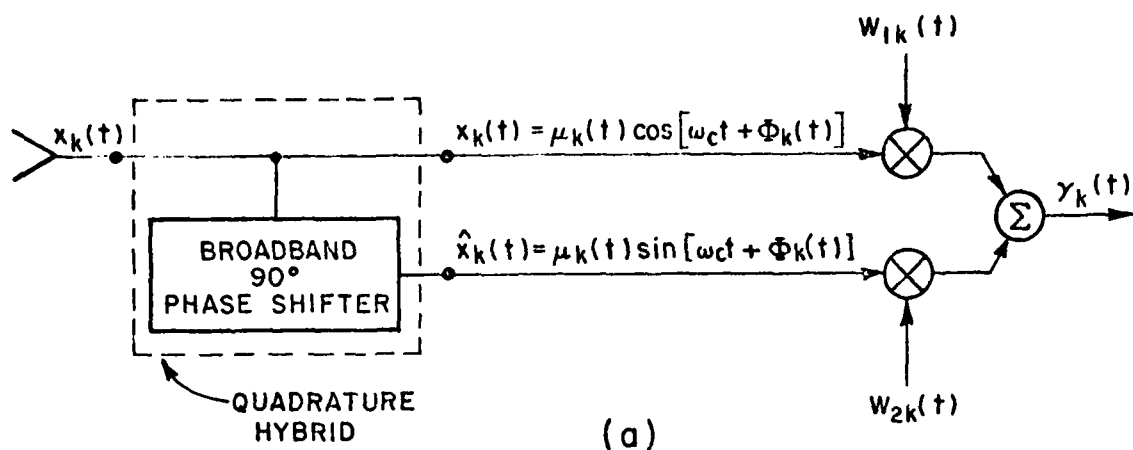
Fig. 2. Weighting coefficient models with
(a) real signals,
(b) complex-envelope signals.

(6)
$$\frac{d\,\underline{w}(t)}{dt} = \alpha\,\underline{\tilde{x}}(t)\,\tilde{e}(t)^\dagger = \alpha\,\overset{\sim}{\underline{x}}(t)\,[\tilde{r}(t) - \overset{\sim}{\gamma}(t)]^\dagger$$

$$= \alpha\,[\overset{\sim}{\underline{x}}(t)\,\tilde{r}(t)^\dagger - \overset{\sim}{\underline{x}}(t)\,\overset{\sim}{\underline{x}}(t)^\dagger\,\underline{w}(t)].$$

In this equation $\tilde{e}(t)$ is the error signal pre-envelope, $\tilde{r}(t)$ is the reference signal pre-envelope, and α is a positive gain constant controlling the speed or response (or bandwidth) of the feedback loops. Figure 3 illustrates the vector processing model defined by Eq. (6).

5

WEIGHTING COEFFICIENT MULTIPLIERS

$\tilde{\underline{x}}(t)$

$\tilde{\gamma}(t) = \underline{w}(t)^{t}\tilde{\underline{x}}(t)$

ADJOINT †

$\underline{w}(t)$

$\int_{t_0}^{t}(\cdot)d\tau$

$\dot{\underline{w}}(t)$

α LOOP GAIN

ADJOINT †

ERROR × INPUT MULTIPLIERS

$\tilde{r}(t)$

ERROR $\tilde{e}(t) = \tilde{r}(t) - \tilde{\gamma}(t)$
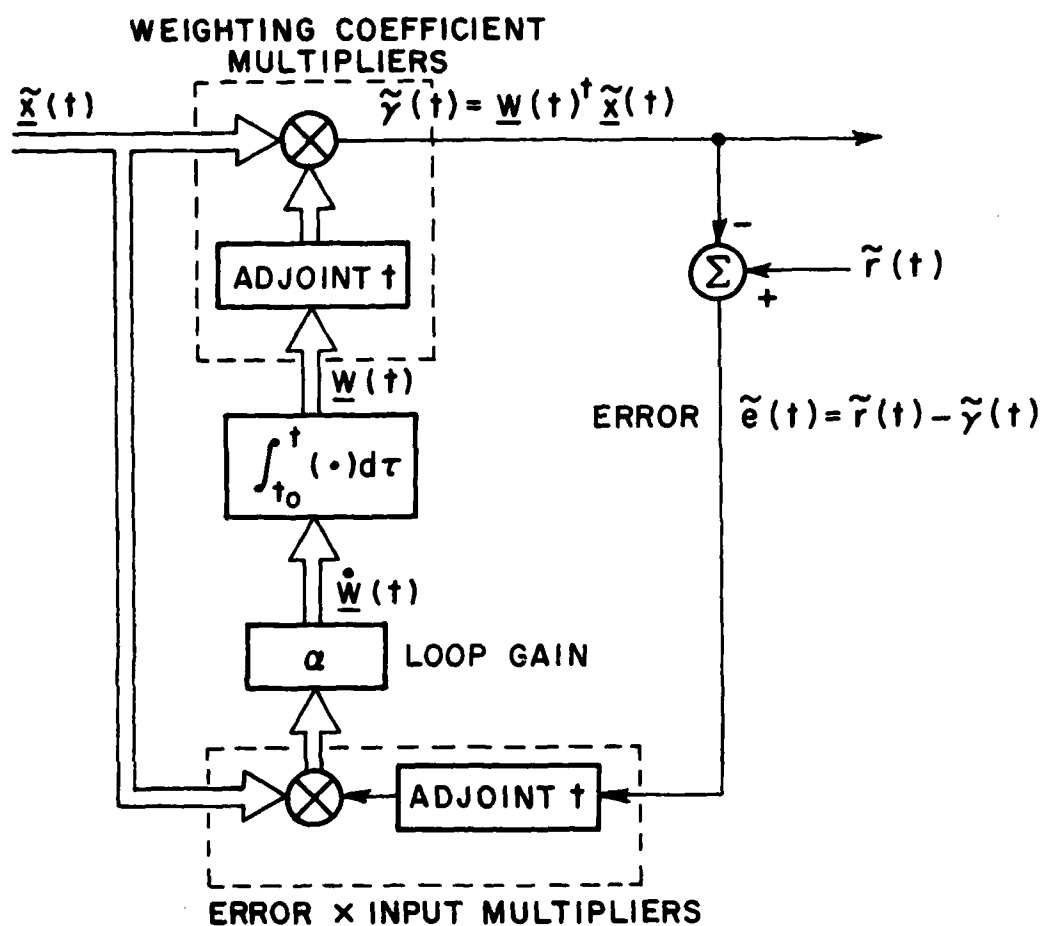
Fig. 3. Adaptive processor model.

For an m-element array, 2m feedback loops are required. Note in Eq. (6) that the error signal's pre-envelope is <u>conjugated</u> implying that phase <u>difference</u> terms of the error-by-signal multiplier outputs are to be <u>retained physically</u>. The double frequency ($2f_c$) components are assumed to be eliminated by low-pass zonal filtering of the error multiplier outputs (not shown in Fig. 3).

Equation (6) is a linear differential equation in $\underline{w}(t)$ with random coefficients, $\underline{\tilde{x}}(t)\,\underline{\tilde{x}}(t)^+$, whose statistics are dependent on the input vector. The expected value of the weight vector response to the input vector satisfies an equation given by the expectation of Eq. (6) over all random variables present:

(7)
$$\frac{1}{\alpha}\frac{d\underline{n}(t)}{dt} = \underline{r}_x - K_x\,\underline{n}(t) - E\left[\{\underline{\tilde{x}}(t)\,\underline{\tilde{x}}(t)^+ - K_x\}\{\underline{w}(t) - \underline{n}(t)\}\right]$$

where $\underline{n}(t) \equiv E[\underline{w}(t)]$ = mean weight vector

$\underline{r}_x \equiv E[\underline{\tilde{x}}(t)\,\underline{\tilde{r}}(t)^+]$ = input-reference crosscorrelation vector

$K_x \equiv E[\underline{\tilde{x}}(t)\,\underline{\tilde{x}}(t)^+]$ = correlation matrix of the input vector.

The latter two terms on the left-hand side of Eq. (7) result from the expectation of the coefficient matrix times the weight vector processes in Eq. (6). It will be necessary to neglect the contribution of the last term in Eq. (7) in the analyses to follow. That is, the assumption of small weight fluctuations about the mean value, $n(t)$, and negligible correlation between weight fluctuations and fluctuations in the instantaneous coefficient matrix will be made. This approximation is valid when the response time of the feedback loop is much larger than the reciprocal of the IF bandwidth, i.e., when loop processing is narrowband in comparison to the modulation bandwidth of the input signal[9,11]. In general, the loop gain constant α can be adjusted to satisfy this condition.

The analysis procedure to be followed consists of adopting suitable models for the structure of the input signals, calculating the correlation matrix K_x and crosscorrelation vector r_x for these models, and solving the approximate equation

(8)
$$\frac{1}{\alpha}\frac{d\underline{n}(t)}{dt} = \underline{r}_x - K_x\,\underline{n}(t)$$

for the asymptotic value of the mean weight vector (as $t\to\infty$). Suitable measures of array performance in steady-state will then be analyzed as a function of the parameters assumed in the models.

B.   Received Signal Model

In this section, explicit representations for the input vector of pre-envelopes and the associated correlation matrix are developed. For analysis purposes an array of ideal antenna elements is assumed, and inter-element time delays are assumed small in comparison to the

7

reciprocal of the received signal bandwidth. With the latter restriction of narrowband signals compared to "array bandwidth", the signals received from a specified direction have identical modulations in the different array elements except for carrier phase shift. The direct (line-of-sight) signal received by the array and the reflected (multipath) signal received by the array are represented as separate vector components of the input vector, Eq. (1), in the expansion

(9)
$$\undertilde{x}(t) = \undertilde{\xi}_1(t)\,\underline{v}_1 + \undertilde{\xi}_2(t)\,\underline{v}_2 + \undertilde{n}(t)$$

where

$\undertilde{\xi}_1(t)$ = pre-envelope of direct signal at the phase center of the array,

$\undertilde{\xi}_2(t)$ = pre-envelope of multipath signal at the phase center of the array,

$\underline{v}_i$ = vector of rf phase shifts associated with the ith signal (i=1 direct; i=2 multipath)

$$= \begin{bmatrix} e^{-j\,\omega_{rf}\,\tau_{i1}} \\ e^{-j\,\omega_{rf}\,\tau_{i2}} \\ \vdots \\ e^{-j\,\omega_{rf}\,\tau_{im}} \end{bmatrix} \quad , \quad i=1,2$$

ω_{rf} = design value of rf carrier frequency

τ_{ik} = incremental path delay from the array phase center to the kth array element in the direction-of-arrival of the ith signal,

$\underline{n}(t)$ = vector of pre-envelopes, $\undertilde{\zeta}_k(t)$, k=1,2,$\cdots$,m of element thermal noise processes.

The incremental time delays, τ_{ik}, in the phase-shift vectors v_i are dependent on array geometry and signal angle-of-arrival. For the special case of an m-element, equispaced linear array of element separation ρ, and a signal incident at β_i degrees from the array axis, the vector v_i is given by

8

$$(10) \quad \underline{v}_i = \begin{bmatrix} e^{j\frac{m-1}{2}\phi_i} \\ \vdots \\ e^{j\,\phi_i} \\ e^{j\,0} \\ e^{-j\,\phi_i} \\ \vdots \\ e^{-j\frac{m-1}{2}\phi_i} \end{bmatrix}_{\text{m-odd}} \quad \text{or} \quad \begin{bmatrix} e^{j\frac{m}{2}\phi_i} \\ \vdots \\ \cdot \\ e^{j\frac{1}{2}\phi_i} \\ e^{-j\frac{1}{2}\phi_i} \\ \vdots \\ e^{-j\frac{m}{2}\phi_i} \end{bmatrix}_{\text{m-even}}$$

where ϕ_i is the electrical phase shift per element at the carrier frequency ω_{rf},

$$\phi_i = 2\pi \frac{\rho}{\lambda_{rf}} \cos \beta_i, \quad i=1,2.$$

As will be shown later, the angular separation of direct and multipath signals appears in the expressions for array performance as an inner product of the phase-shift vectors v_1 and v_2:

$$(11) \quad <\underline{v}_1,\underline{v}_2> = \sum_{k=1}^{m} e^{j\omega_{rf}(\tau_{1k}-\tau_{2k})}.$$

For equispaced linear arrays, the summation in Eq. (11) is dependent only on the difference in electrical phase shift per element $(\phi_1-\phi_2)$, i.e.,

$$(12) \quad <\underline{v}_1,\underline{v}_2> = \frac{\sin(\frac{m\psi}{2})}{\sin(\frac{\psi}{2})} \quad ; \quad \psi = 2\pi\frac{\rho}{\lambda_{rf}}[\cos\beta_1-\cos\beta_2].$$

A purely specular model for the multipath signal is adopted in this study. The direct and multipath signal pre-envelopes in Eq. (9) will be assumed to be represented by the functions

9

$$(13) \qquad \tilde{\xi}_1(t) = \sqrt{S} \, e^{j[p(t) + \Delta\omega_1 t + \theta_1]}$$

$$\tilde{\xi}_2(t) = \sqrt{M} \, e^{j[p(t-\varepsilon_m) + \Delta\omega_2 t + \theta_2]}$$

where

$\sqrt{S}$ = rms amplitude of direct component

$\sqrt{M}$ = rms amplitude of reflected component

$p(t)$ = angle modulation of direct component

ε_m = differential path delay of reflected component relative to direct component

$\Delta\omega_{1,2}$ = carrier frequency offsets from the design value

$\theta_{1,2}$ = carrier phase angles at the array phase center.

Frequency offsets representing carrier frequency uncertainties or drift and/or doppler frequency shift are included in the above representations for the sake of completeness. The effects of these offsets on array response will not be determined in the present study, however, due to difficulties encountered in the analysis; i.e., these offsets will be set equal to zero later.* All time-independent parameters of the signals in Eq. (13) are assumed to be non-random. The angle modulation $p(t)$ will be modeled as a random process which includes the transmitted information modulation (data) plus any subcarrier phase modulation (code) added for bandspreading purposes. The pre-envelope of the transmitted signal, $\exp[j\, p(t)]$, will be defined to have a stationary ensemble autocorrelation function

$$(14) \qquad R_p(\tau) \equiv E[e^{j\, p(t)} \, e^{-j\, p(t-\tau)}].$$

A particular type of phase modulation of special interest is that employed in coded, binary communications systems. The communications signal is generated by bi-phase modulating a carrier signal with the modulo-two sum of a random binary data sequence and a pseudonoise (PN) code. This signal will be modeled as the product of two independent

---

*A closed-form asymptotic solution to the differential equation, Eq. (8), has not been found for the case of non-zero frequency offsets.

10

random binary processes with bit periods of T_b and Δ seconds which correspond, respectively, to the data and code bit durations. The autocorrelation function of this signal is a product of triangular functions:

$$(15) \qquad R_p(\tau) = \begin{cases} (1 - \frac{|\tau|}{\Delta})(1 - \frac{|\tau|}{T_b}) & , \ |\tau| < \Delta \\[2em] 0 & , \ |\tau| \geq \Delta \end{cases}$$

$$(\Delta < T_b).$$

The autocorrelation and crosscorrelation functions of the signals present at the receiving array are calculated from Eq. (13) as follows:

$$(16) \qquad E[\tilde{\xi}_1(t) \, \tilde{\xi}_1(t-\tau)^\dagger] = S \, e^{j\Delta\omega_1} \, R_p(\tau)$$

$$E[\tilde{\xi}_2(t) \, \tilde{\xi}_2(t-\tau)^\dagger] = M \, e^{j\Delta\omega_2\tau} \, R_p(\tau)$$

$$E[\tilde{\xi}_1(t) \, \tilde{\xi}_2(t-\tau)^\dagger] = \sqrt{SM} \, e^{j[(\Delta\omega_1-\Delta\omega_2)t + \Delta\omega_2\tau + \theta_1-\theta_2]}$$

$$\cdot R_p(\tau + \epsilon_m).$$

The crosscorrelation function in the last expression is non-stationary when the differential doppler shift ($\Delta\omega_1 - \Delta\omega_2$) between direct and multipath signals is non-zero.

The thermal noise processes in Eq. (9) are assumed to Gaussian, stationary, and independent of each other and the received signals. These noise processes are assumed to have a constant power spectral density, N_0, over the noise bandwidth, B_{if}, of the IF amplifiers. The correlation matrix associated with the input thermal noise vector is given by the diagonal matrix

$$(17) \qquad E[\underline{\tilde{n}}(t) \, \underline{\tilde{n}}(t)^\dagger] = \sigma^2 \, I,$$

where $\qquad \sigma^2 = B_{if} N_0$

is the mean-square amplitude of each noise process. (I is the identity matrix.)

Consider now the calculation of the correlation matrix, K_x. For narrowband input vectors, as in Eq. (9), this matrix is given by

(18)
$$K_x = E[\tilde{\underline{x}}(t)\, \tilde{\underline{x}}(t)^\dagger]$$

$$= E[|\tilde{\xi}_1(t)|^2]\, \underline{v}_1\underline{v}_1{}^\dagger + E[|\xi_2(t)|^2]\, \underline{v}_2\underline{v}_2{}^\dagger$$

$$+ E[\tilde{\xi}_1(t)\, \tilde{\xi}_2(t)^\dagger]\, \underline{v}_1\underline{v}_2{}^\dagger + E[\tilde{\xi}_2(t)\, \tilde{\xi}_1(t)^\dagger]\, \underline{v}_2\underline{v}_1{}^\dagger$$

$$+ E[\tilde{\underline{n}}(t)\, \tilde{\underline{n}}(t)^\dagger].$$

In this result, a dyadic matrix $v_i v_i{}^\dagger$ is present corresponding to each input signal, and a pair of adjoint matrices, $v_i v_j{}^\dagger$ and $v_j v_i{}^\dagger$, is present due to the crosscorrelation of the ith and jth input signals. For the particular model represented by Eqs. (13)-(17), the correlation matrix has the form

(19)
$$K_x(t) = S\, \underline{v}_1\underline{v}_1{}^\dagger + M\, \underline{v}_2\underline{v}_2{}^\dagger$$

$$+ \sqrt{SM}\, R_p(\epsilon_m)\, e^{j(\omega_{12}t + \theta_{12})}\, \underline{v}_1\underline{v}_2{}^\dagger$$

$$+ \sqrt{SM}\, R_p(\epsilon_m)^\dagger\, e^{-j(\omega_{12}t + \theta_{12})}\, \underline{v}_2\underline{v}_1{}^\dagger$$

$$+ \sigma^2\, I$$

where
$$\omega_{12} \equiv \Delta\omega_1 - \Delta\omega_2$$
$$\theta_{12} \equiv \theta_1 - \theta_2.$$

This correlation matrix has elements which vary periodically with time; the frequency of repetition is equal to the differential doppler frequency shift between direct and multipath signals.

C.   Array Reference Signal Model

Ideally, the reference signal for the array is a replica of the desired signal component in the array output. The error signal in this case contains only undesired components, and the feedback processing acts to remove these components from the array output. In practice,

however, an ideal reference signal cannot be generated since received signal parameters may not be known precisely and unknown (data) modulation may be present in the received signal. Practical techniques for obtaining the reference signal from the array output signal through appropriate waveform processing operations have recently been developed for the case in which the desired signal is a coded, biphase-modulated communication signal[12,13,14]. Similar techniques which use a "bootstrap" reference loop to generate an estimate of the desired received signal have been investigated experimentally for the case of FSK modulation[15]. Although the reference signal obtained using these approaches is imperfect, due to practical limitations, there is considerable analytical and experimental evidence which indicates that the effect of these imperfections may be minimized through appropriate design[13].

In the present study, the reference signal will be modeled as a non-processed signal which is independent of the array weighting coefficients and which contains the angle modulation of the input signal to within a timing error, ε_r, and a carrier frequency offset, $\Delta\omega_r$:

$$(20) \qquad \tilde{r}(t) = \sqrt{R}\, e^{j[p(t-\varepsilon_r) + \Delta\omega_r t + \theta_r]}.$$

The timing error parameter in this representation may be varied for perfect time-base alignment with the direct signal ($\varepsilon_r=0$), or multipath signal ($\varepsilon_r=\varepsilon_m$), or for partial alignment near these values of delay. The input-reference crosscorrelation vector may be calculated from Eqs. (9), (13), (14), and (20) as

$$(21) \qquad \underline{r}_x(t) = E[\overset{\sim}{\underline{x}}(t)\,\tilde{r}(t)^{+}] =$$

$$\sqrt{RS}\, e^{j[(\Delta\omega_1-\Delta\omega_r)t + (\theta_1-\theta_r)]}\, R_p(\varepsilon_r)\, \underline{v}_1$$

$$+ \sqrt{RM}\, e^{j[(\Delta\omega_2-\Delta\omega_r)t + (\theta_2-\theta_r)]}\, R_p(\varepsilon_r-\varepsilon_m)\, \underline{v}_2 \ .$$

The components of this vector along the vectors v_1 and v_2 vary periodically in time at unequal rates in general. Only in the special cases where $\Delta\omega_r=\Delta\omega_1$ or $\Delta\omega_r=\Delta\omega_2$ is there a single frequency of periodicity which matches that of the correlation matrix. These choices simplify the task of finding the forced response of the system, Eq. (8); however, the basic problem of finding solutions to the homogeneous system ($r_x=0$) containing the periodically stationary

13

matrix, Eq. (19), is not affected. In the next chapter, closed-form solutions are presented only for the limiting case of zero frequency offsets:

$$\Delta\omega_1 = \Delta\omega_2 = \Delta\omega_r = 0.$$

III. PERFORMANCE ANALYSES

A. Mean Weight Vector Response

For the case where all carrier frequency offsets in the model are assumed to equal zero, the mean weight vector equation, Eq. (8), assumes the form

$$(22) \qquad \frac{1}{\alpha} \frac{d\underline{n}(t)}{dt} = A \underline{v}_1 + B \underline{v}_2$$

$$- \left\{ S \underline{v}_1\underline{v}_1^{+} + M \underline{v}_2\underline{v}_2^{+} + \sigma^2 I \right.$$

$$\left. + C \underline{v}_1\underline{v}_2^{+} + C^{+} \underline{v}_2\underline{v}_1^{+} \right\}\underline{n}(t)$$

where

$$A = \sqrt{R}\sqrt{S} \; R_p(\epsilon_r) \; e^{j(\theta_1-\theta_r)}$$

$$B = \sqrt{R}\sqrt{M} \; R_p(\epsilon_r-\epsilon_m) \; e^{j(\theta_2-\theta_r)}$$

$$C = \sqrt{S}\sqrt{M} \; R_p(\epsilon_m) \; e^{j\theta_{12}} \quad .$$

The asymptotic solution to Eq. (22) is

$$\left. \frac{d\underline{n}(t)}{dt} \right|_{t\to\infty} = 0$$

$$\left. \underline{n}(t) \right|_{t\to\infty} = K_x^{-1} \underline{r}_x$$

$$= \left\{ \begin{array}{l} S \underline{v}_1\underline{v}_1^{+} + M \underline{v}_2\underline{v}_2^{+} + \sigma^2 I \\ + C \underline{v}_1\underline{v}_2^{+} + C^{+} \underline{v}_2\underline{v}_1^{+} \end{array} \right\}^{-1} (A \underline{v}_1 + B \underline{v}_2).$$

14

The inverse matrix can be calculated analytically using the Woodbury identity as discussed in Reference [13]. A simpler approach yielding identical results is to substitute into Eq. (22) the trial solution

(23)
$$\underline{n}(t)\big|_{t\to\infty} = a\,\underline{v}_1 + b\,\underline{v}_2 \,, \qquad \frac{d\underline{n}(t)}{dt}\Big|_{t\to\infty} = \underline{0} \,.$$

This substitution yields a linear combination of the vectors v_1 and v_2 on the right-hand side of the equation and the zero vector on the left-hand side. The vectors v_1 and v_2 are linearly independent in general. Algebriac dependence of v_1 and v_2 occurs only when the differential delays, τ_{ik}, in Eq. (11) satisfy a very special set of relationships. Thus, the coefficients multiplying v_1 and v_2 in the left-hand side of Eq. (22) may be set to zero individually yielding a pair of simultaneous algebraic equations in the unknown coefficients of Eq. (23):

$$(mS+\sigma^2+C<v_2,v_1>)\,a + (mC+S<v_1,v_2>)\,b = A$$

$$(mC^++M<v_2,v_1>)\,a + (mM+\sigma^2+C^+<v_1,v_2>)\,b = B.$$

The solution of this system is

(24)
$$a = \frac{A(mM+\sigma^2+C^+<v_1,v_2>)-B(mC+S<v_1,v_2>)}{|D|}$$

$$b = \frac{B(mS+\sigma^2+C<v_2,v_1>)-A(mC^++M<v_2,v_1>)}{|D|}$$

where the system determinant, $|D|$, is given by

(25)
$$|D| = m^2 SM\left(1 - |R_p(\epsilon_m)|^2\right)\left(1 - \frac{|<v_1,v_2>|^2}{m^2}\right)$$

$$+ \sigma^2\left[m(S+M) + 2\sqrt{S M}\,\mathrm{Re}\left\{e^{j\theta_{12}} R_p(\epsilon_m)<v_2,v_1>\right\}\right]$$

$$+ \sigma^4 \,.$$

15

The effect of multipath interference is an alteration of the relative magnitudes of weight vector components along the vectors v_1 and v_2. This is reflected by the presence of the coefficients B and C in the expressions of Eq. (24). These coefficients are equal to zero when the input interfering signal is uncorrelated with the desired (direct) input signal.

B. Output Signal Mean Phase

In this section the mean phase of the array output signal is calculated for the case where the mean weight vector approaches its steady-state value in Eq. (23). The first question of interest is whether or not the mean phase approaches the mean phase of the reference signal when the output signal consists of two correlated components. The asymptotic form of the output signal is given by

$$(26) \qquad \tilde{\gamma}_s(t)\Big|_{t \to \infty} = \underline{n}(\infty)^\dagger \{\tilde{\xi}_1(t) \, \underline{v}_1 + \tilde{\xi}_2(t) \, \underline{v}_2\}$$

$$= \underline{n}(\infty)^\dagger \left\{ \sqrt{S} \, e^{j[p(t)+\theta_1]} \, \underline{v}_1 + \sqrt{M} \, e^{j[p(t-\epsilon_m)+\theta_2]} \, \underline{v}_2 \right\}$$

$$= e^{j[p(t-\epsilon_r)+\theta_r]} \, Q(t)$$

$$\text{where} \qquad Q(t) = \underline{n}(\infty)^\dagger \underline{v}_1 \, \sqrt{S} \, e^{j(\theta_1-\theta_r)} \left\{ e^{j[p(t)-p(t-\epsilon_r)]} \right\}$$

$$+ \underline{n}(\infty)^\dagger \underline{v}_2 \, \sqrt{M} \, e^{j(\theta_2-\theta_r)} \left\{ e^{j[p(t-\epsilon_m)-p(t-\epsilon_r)]} \right\}.$$

The two terms comprising $Q(t)$ are complex constants when the time delays ϵ_m and ϵ_r are zero, and are complex random processes otherwise. The expectation of $Q(t)$ represents the average amplitude and phase (relative to θ_r) of that portion of the array output signal which is correlated with the reference signal. This expectation is given by

$$(28) \qquad E\left\{ \tilde{\gamma}_s(t) \, e^{-j[p(t-\epsilon_r)+\theta_r]} \right\}\Bigg|_{t \to \infty} = E[Q(t)]\Big|_{t \to \infty}$$

$$= \underline{n}(\infty)^\dagger \underline{v}_1 \, \sqrt{S} \, e^{j(\theta_1-\theta_r)} \, R_p(\epsilon_r)$$

$$+ \underline{n}(\infty)^\dagger \underline{v}_2 \, \sqrt{M} \, e^{j(\theta_2-\theta_r)} \, R_p(\epsilon_r-\epsilon_m)$$

16

where the inner products involving the mean weight vector are evaluated as shown below.

(29) $\underline{n}(\infty)^{\dagger}\underline{v}_1 = ma^{\dagger} + <v_2,v_1>b^{\dagger}$

$$= (m^2 - |<v_1,v_2>|^2)\frac{(MA^{\dagger}-B^{\dagger}C^{\dagger})}{|D|} + m\sigma^2\frac{A^{\dagger}}{|D|}$$

$$+ <v_2,v_1>\sigma^2\frac{B^{\dagger}}{|D|} ;$$

(30) $\underline{n}(\infty)^{\dagger}\underline{v}_2 = (m^2 - |<v_1,v_2>|^2)\frac{(SB^{\dagger}-A^{\dagger}C)}{|D|} + m\sigma^2\frac{B^{\dagger}}{|D|}$

$$+ <v_1,v_2>\sigma^2\frac{A^{\dagger}}{|D|} .$$

Each inner product consists of the sum of three complex numbers whose arguments are given by one of two possible values:

(31)
$$\underline{/A^{\dagger}} = \underline{/B^{\dagger}C^{\dagger}} = \theta_r - \theta_1$$
$$\underline{/B^{\dagger}} = \underline{/A^{\dagger}C} = \theta_r - \theta_2$$

This result follows from the definitions for the parameters A, B, and C in Eq. (22) when the complex autocorrelation function $R_p(\tau)$ is a real-valued function of τ. This conditon will be satisfied for balanced types of digital phase modulation p(t) whose allowed phase states are symmetrically distributed over $(0, 2\pi)$ and occur with equal probability. The inner product of vectors v_1 and v_2 in Eqs. (29) and (30) is real-valued, as noted in Eq. (12), when the reference point for signal representation is chosen at the array phase center. Thus, the first term of Eq. (28), the direct signal contribution, is comprised of three components of which the first two are real-valued. The remaining component has its argument along $(\theta_1-\theta_2)$ and is given by

$$<v_2,v_1>\sigma^2\frac{\sqrt{R}\sqrt{M}\sqrt{S}}{|D|} R_p(\epsilon_r-\epsilon_m) R_p(\epsilon_r) e^{j(\theta_1-\theta_2)} .$$

17

The same conclusions are true for the second term in Eq. (28) -- the multipath contribution -- with the exception that the phase argument of the third component is along $(\theta_2-\theta_1)$:

$$\langle v_1,v_2\rangle \sigma^2 \frac{\sqrt{R}\sqrt{S}\sqrt{M}}{|D|} \; R_p(\varepsilon_r) \; R_p(\varepsilon_r-\varepsilon_m) \; e^{j(\theta_2-\theta_1)} \quad .$$

Upon comparing the above expressions, it can be concluded that the third components are a conjugate pair; hence, their sum is real-valued which implies that Eq. (28) is real-valued. Figure 4 shows a phasor
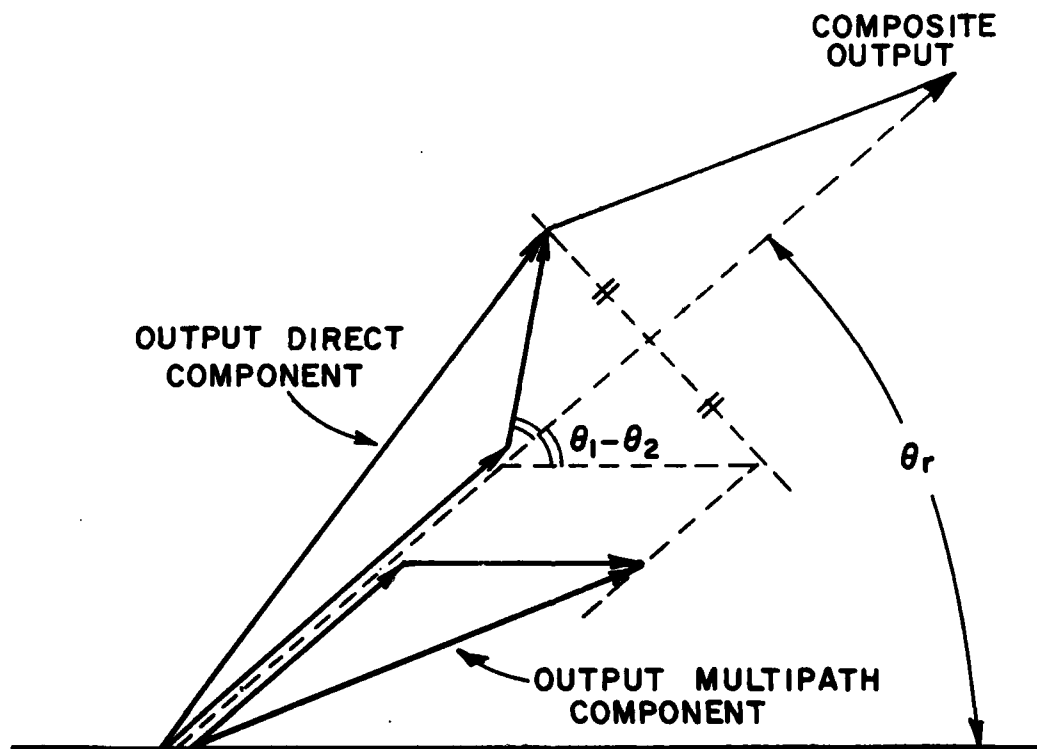

Fig. 4. Mean amplitude and phase of direct and multipath components in array output.

18

diagram of the components of Eq. (28) where each component has been rotated counterclockwise by θ_r degrees. These results indicate that the steady-state composite output signal is phase-aligned with the reference signal on the average whereas its components, the direct and multipath output signals, are not.

The composite output signal in Eq. (26) may also be separated into a component which is completely correlated with the reference signal plus a component which is uncorrelated with the reference signal:

$$(32) \qquad \tilde{\gamma}_s(t)\Big|_{t\to\infty} = e^{j[p(t-\epsilon_r) + \theta_r]} E[Q(t)]$$
$$+ e^{j[p(t-\epsilon_r) + \theta_r]} \{Q(t) - E[Q(t)]\} \quad .$$

The second term in this expression represents the uncorrelated output component. The correlated output component contains the correlated "portion" of both the direct and multipath signals at the array output while the uncorrelated component contains the remainder of these signals. The importance of this decomposition is that the uncorrelated output component is not usable for data detection when the time-base of a demodulator following the array is synchronized with the time-base of the reference signal. A discussion of post-array data demodulation is given later in Section III-D.

C.   Output Multipath-to-Direct Signal Ratio

One indicator of array performance is the ratio of powers in the direct and multipath signal components at the array output. With the definition of power in a signal component as the mean-square amplitude of its associated pre-envelope, the output multipath-to-direct signal power ratio is given by

$$(33) \qquad \frac{P_M}{P_S}(t) \equiv \frac{E|\underline{w}(t)^\dagger \tilde{\xi}_2(t)\underline{v}_2|^2}{E|\underline{w}(t)^\dagger \tilde{\xi}_1(t)\underline{v}_1|^2} \doteq \frac{M}{S} \frac{|\underline{n}(t)^\dagger \underline{v}_2|^2}{|\underline{n}(t)^\dagger \underline{v}_1|^2} \quad .$$

The approximation made on the right-hand side of this equation neglects the effects of jitter in the weight vector about its expected value, $n(t)$. From the results in Eqs. (29) and (30), the asymptotic value of this ratio as the mean weight vector settles to its final value is

19

$$(34) \qquad \frac{P_M}{P_S} = \frac{M|<v_1,v_2>\sigma^2 A^\dagger + m\sigma^2 B^\dagger + (m^2 - |<v_1,v_2>|^2)(SB^\dagger - A^\dagger C)|^2}{S|m\sigma^2 A^\dagger + <v_2,v_1>\sigma^2 B^\dagger + (m^2 - |<v_1,v_2>|^2)(MA^\dagger - B^\dagger C^\dagger)|^2}$$

$$= \frac{M}{S} \frac{\left| \frac{<v_1,v_2>}{m} + \frac{B^\dagger}{A^\dagger} + \left(1 - \frac{<v_1,v_2>^2}{m^2}\right)m\sigma^{-2}\left(S\frac{B^\dagger}{A^\dagger} - C\right)\right|^2}{\left| 1 + \frac{<v_2,v_1>}{m}\frac{B^\dagger}{A^\dagger} + \left(1 - \frac{<v_1,v_2>^2}{m^2}\right)m\sigma^{-2}\left(M - \frac{B^\dagger}{A^\dagger}C^\dagger\right)\right|^2} .$$

The computer program in Appendix A was written to evaluate this ratio under the assumption that the signal autocorrelation was given by Eq. (15) with $T_b \gg \Delta$, i.e.,

$$(35) \qquad R_p(\tau) = \begin{cases} 1 - \frac{|\tau|}{\Delta} &, \quad |\tau| < \Delta \\[2mm] 0 &, \quad |\tau| \geq \Delta \end{cases} .$$

A four-element linear array was assumed in the program, using Eq. (12) with m=4. The results are shown in Figs. 5-11.

Figure 5 illustrates performance as a function of the multipath delay, ϵ_m, expressed in PN chip durations (Δ = one code chip), for several values of the angular separation parameter ψ. The input signals are equal in amplitude and the reference signal is perfectly synchronized with the direct component (ϵ_r=0). The carrier phase difference (θ_1-θ_2) is zero in this set of curves. As the multipath delay increases from a small value, the multipath component is increasingly rejected by the array. For multipath delays exceeding one PN chip duration, the array treats the multipath signal the same as it would any uncorrelated interference. The abrupt change in the slope of the curves at the transition point (one chip delay) is attributed to the abrupt change in slope of the triangular autocorrelation function at its base. As might be expected, a multipath signal more widely separated in angle from the direct signal experiences greater suppression at the array output.*

---

*An angular separation of signals of one-half the natural half-power beamwidth of the array corresponds to a value of ψ of approximately 41 electrical degrees.

Fig. 5. Multipath-to-desired signal ratio at array output.

21

Fig. 6. Multipath-to-desired signal ratio at array output.

Fig. 7. Multipath-to-desired signal ratio at array output.
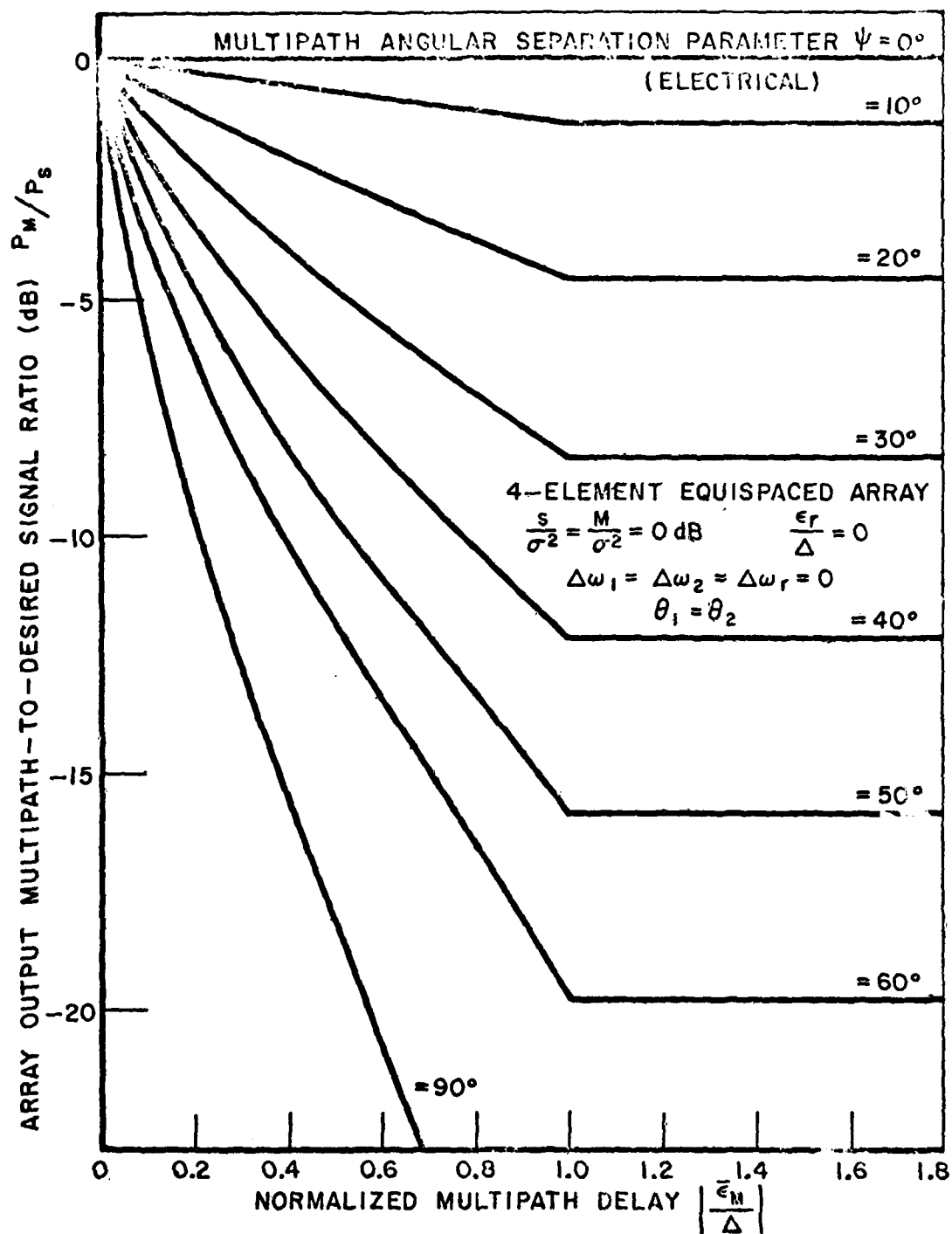
23

Fig. 8. Multipath-to-desired signal ratio at array output.
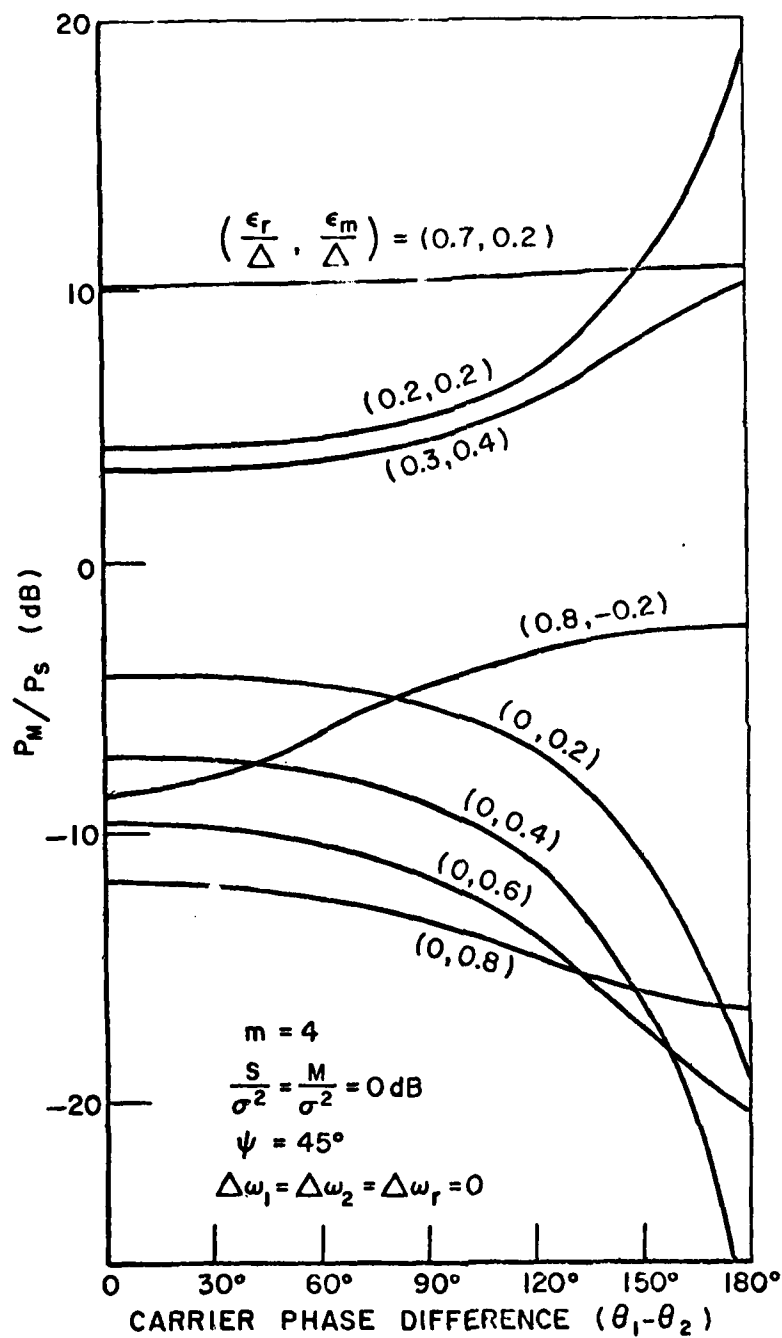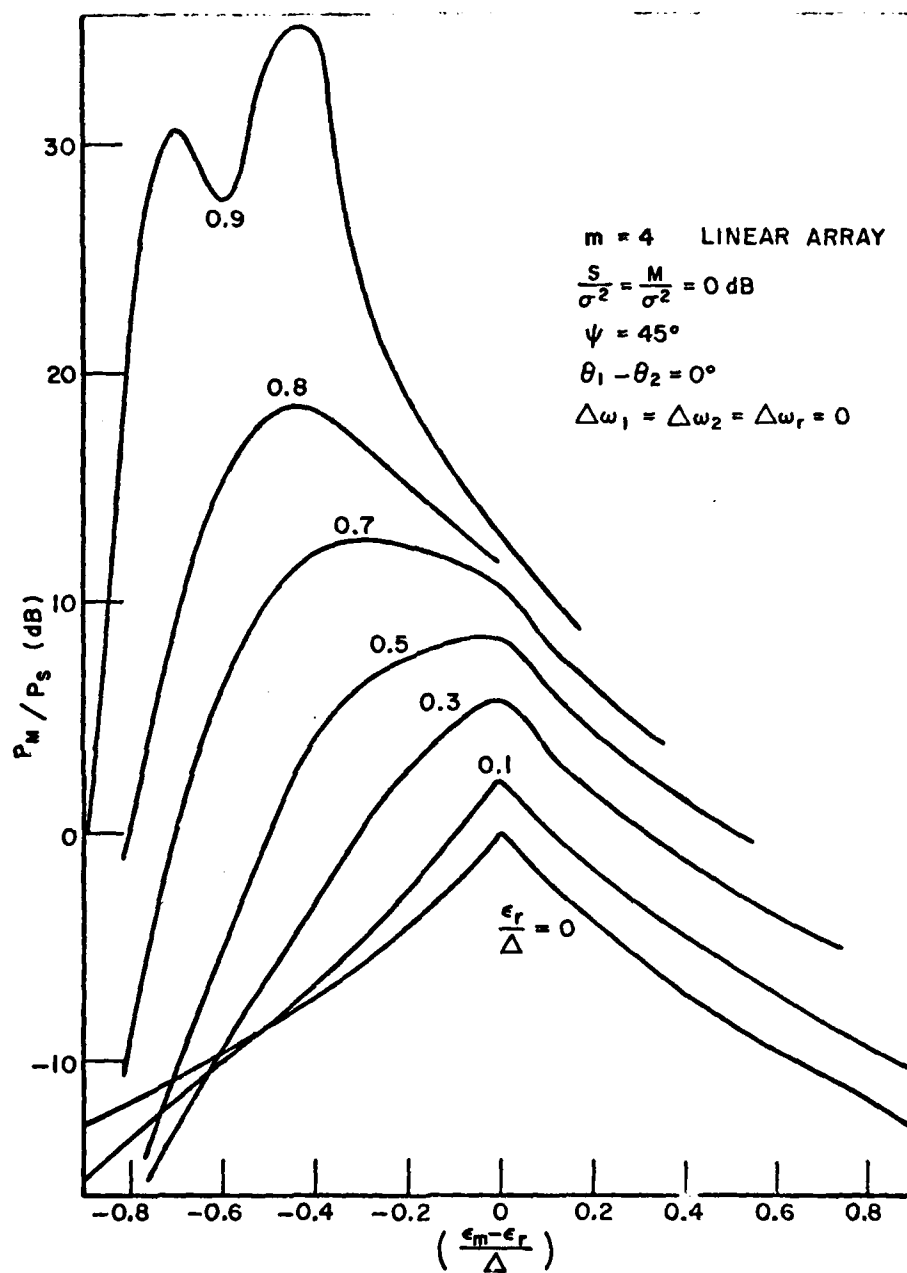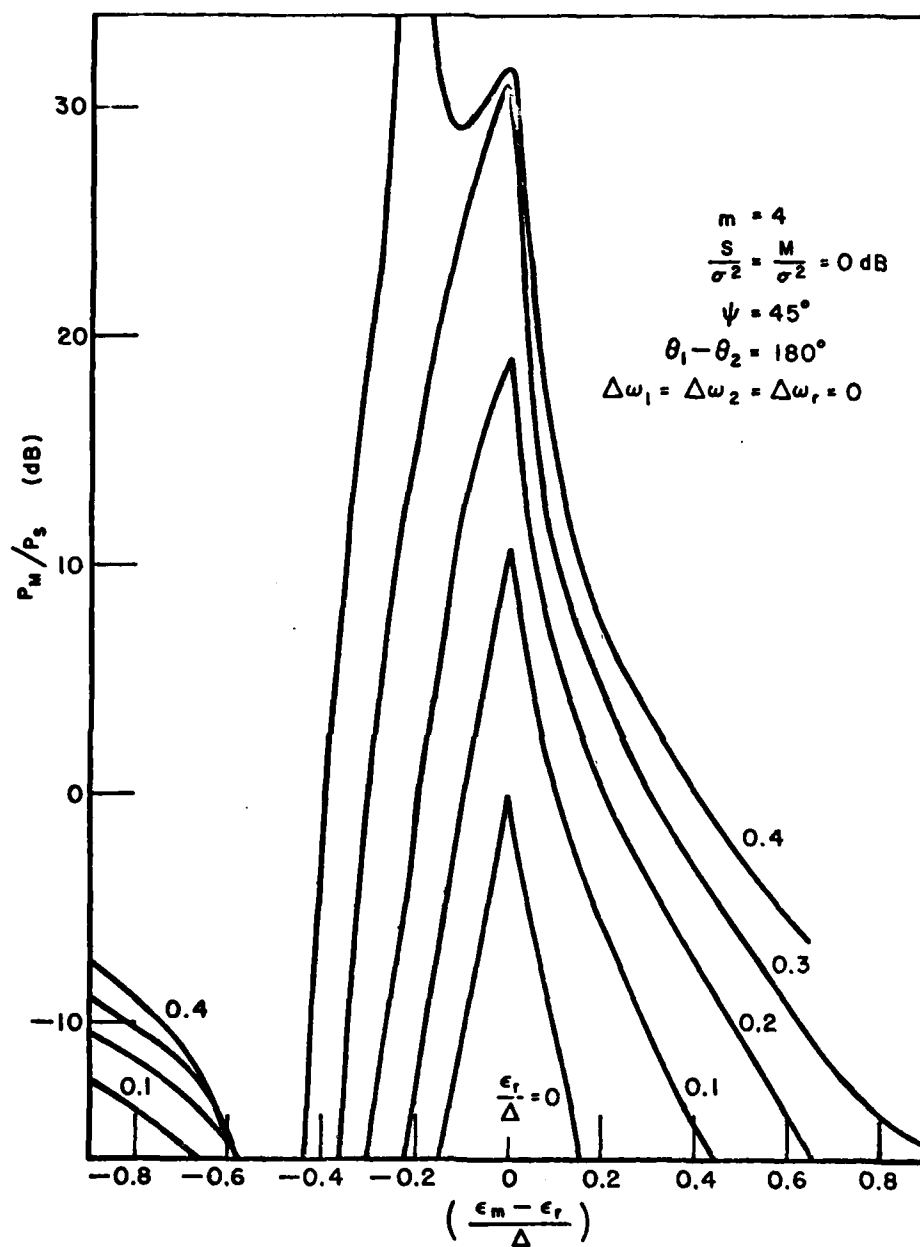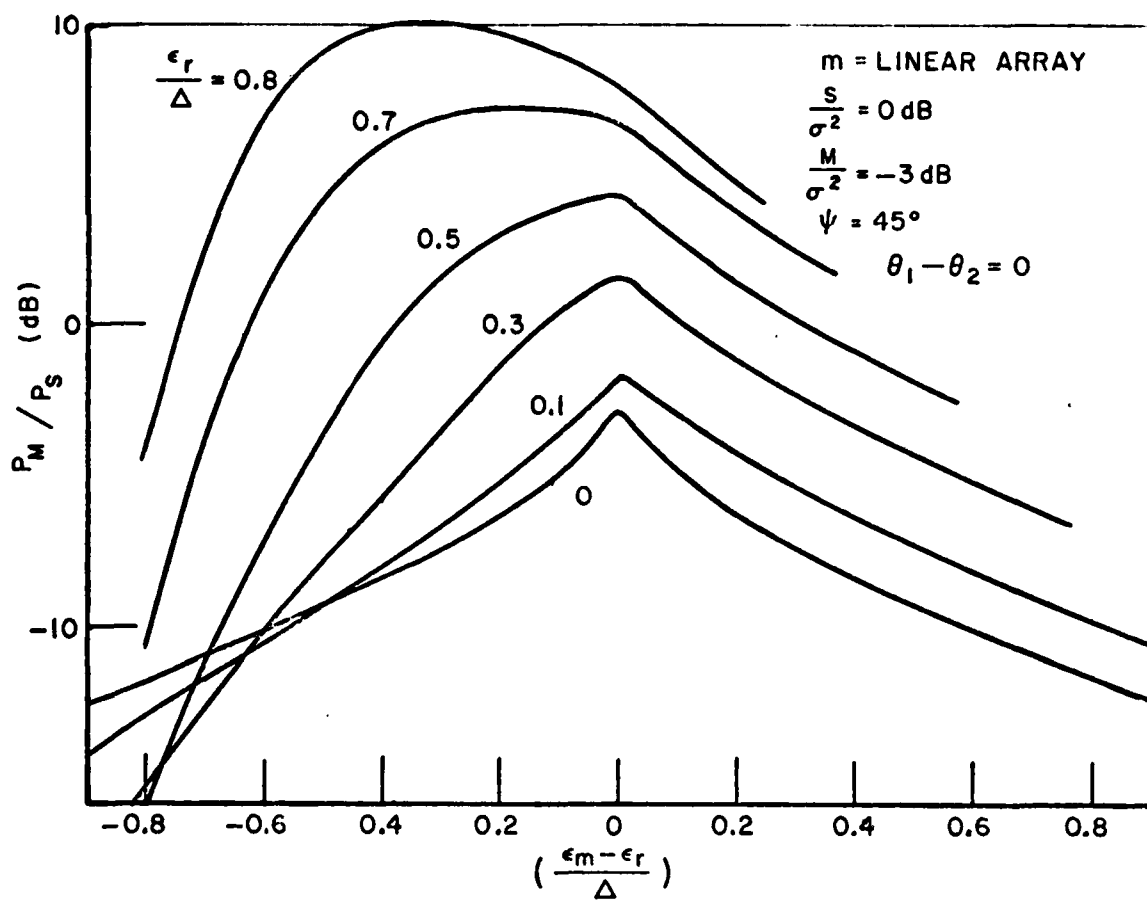
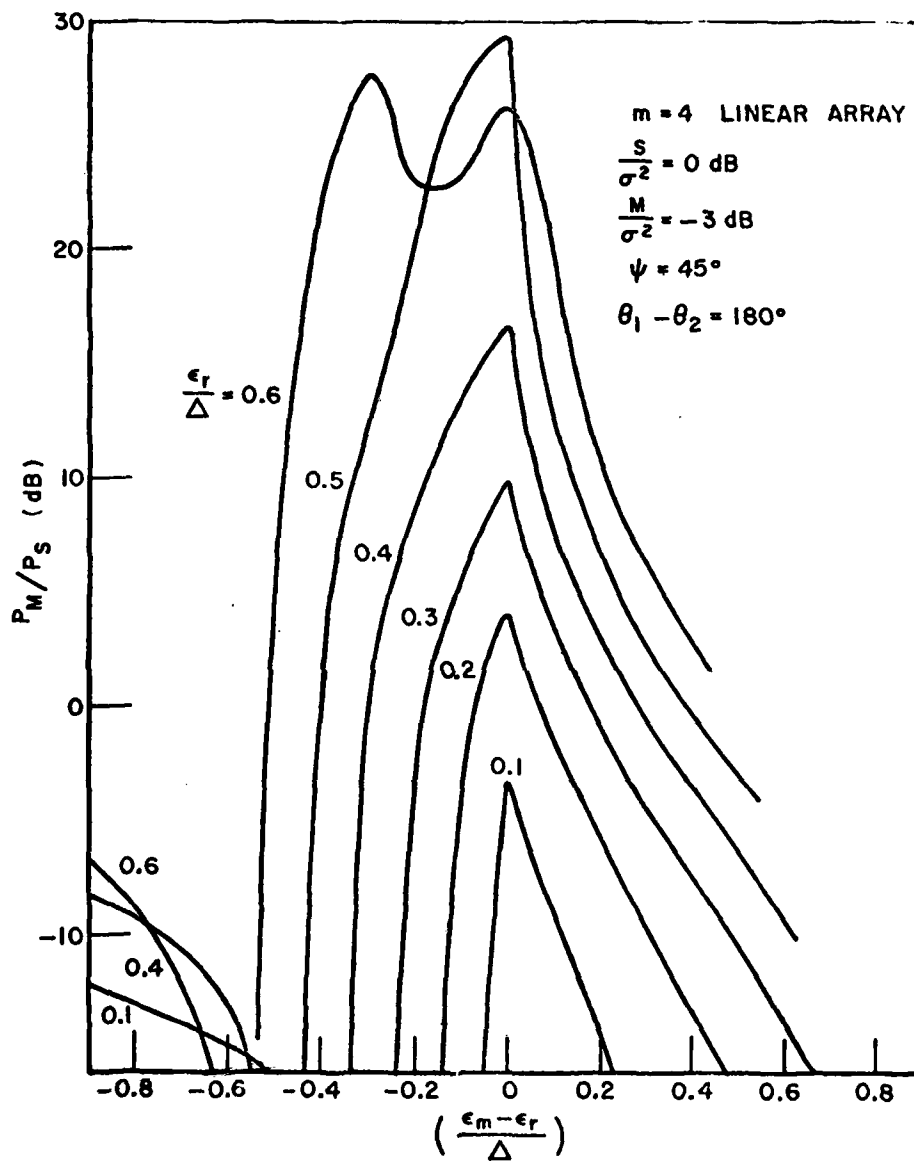Fig. 9. Multipath-to-desired signal ratio at array output.

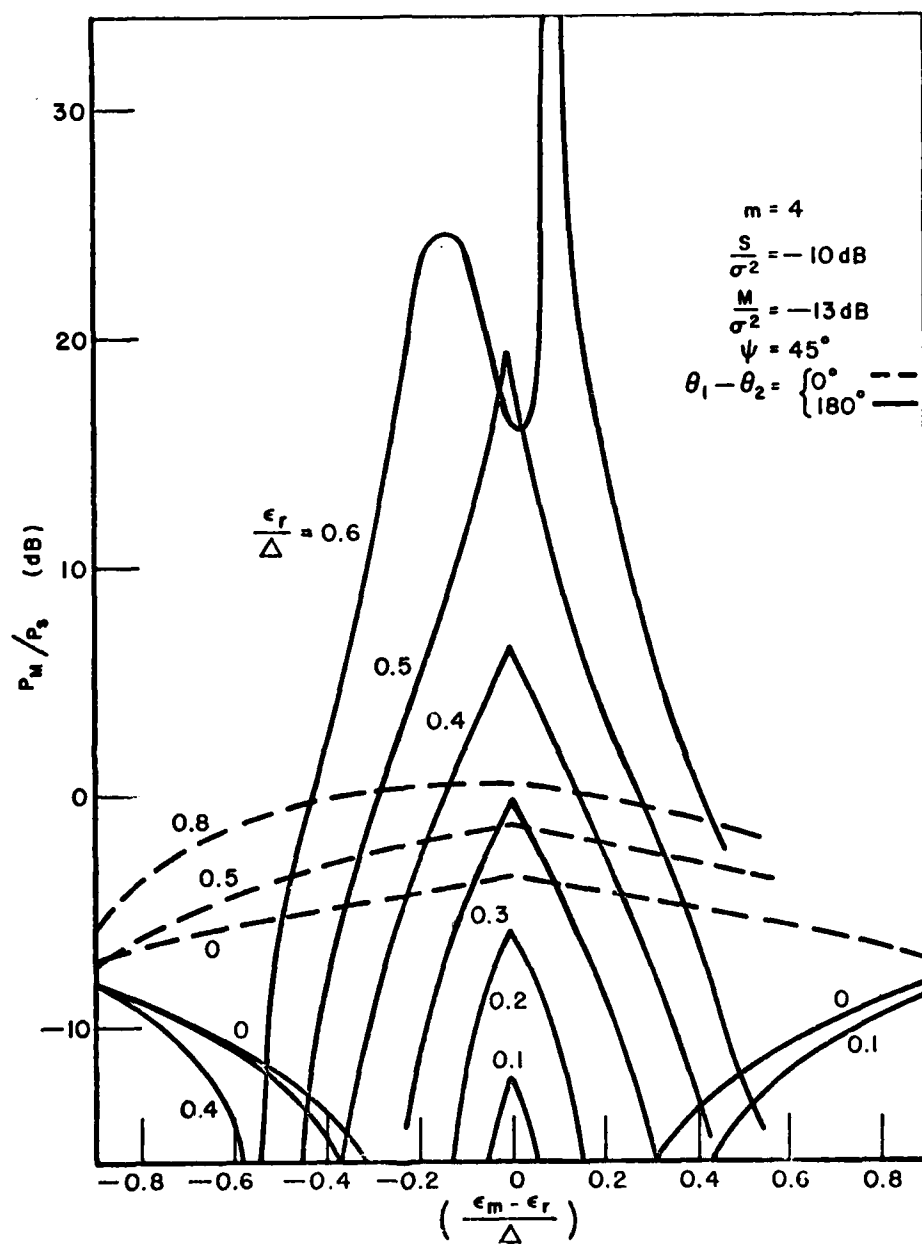Fig. 10. Multipath-to-desired signal ratio at array output.

Fig. 11. Multipath-to-desired signal ratio at array output.

27

Figure 6 illustrates the variation in Eq. (34) versus the carrier phase difference of the input signals. Several curves are shown for different values of multipath delay and reference timing error. Note that each of these curves has a maximum and a minimum at the endpoints, i.e., when the carrier phase difference is either 0° or 180°. Thus,the output ratio is bounded by its values at these two values of carrier phase for specified values of the other input parameters. It can be shown analytically that the derivative of Eq. (34) with respect to carrier phase difference is zero at these values. The proof is lengthy, however, and will not be presented here. Although the results in Fig. 6 apply to the steady-state behavior of the output ratio versus carrier phase difference, they are also expected to be valid when the carrier phase difference $(\theta_1-\theta_2)$ is varying slowly as a function of time. That is, for very small differential doppler shift between input components compared to the reciprocal time constants of the feedback loops, the variation in the output ratio is expected to be that given in Fig. 6 where the abscissa represents a time interval equal to one-half the period of the differential doppler frequency. In essence, the feedback loops "track" the carrier phase increments and maintain optimum "steady-state" performance at each instant of time in this case.

The results in Figs. 7 and 8 indicate that the output ratio is very sensitive to small changes in the timing error parameters. The ratio is plotted versus multipath-reference relative timing error; an abscissa value of zero corresponds to perfect synchronization of these two signals. The parameter distinguishing the different curves is the timing error between direct and reference signals. The direct component is suppressed at the array output when its alignment with the reference is relatively poor, e.g., when

$$\frac{\epsilon_r}{\Delta} = .9 \quad , \quad \frac{\epsilon_m - \epsilon_r}{\Delta} = - .4$$

in Fig. 7. The sensitivity of the output ratio to timing error parameters is more extreme when the carrier phase difference is 180° as indicated by the results in Fig. 8. In Figs. 9 and 10, the amplitude of the multipath component has been reduced by 3 dB at the array input. The curves in these figures have the same basic shape as those in Figs. 7 and 8 but are more closely spaced. The same type of behavior is noted in Figs. 10 and 11 where input signal powers have been reduced by 10 dB relative to thermal noise power.

D.   Usable Output Signal-to-Noise Ratio

The results of the preceding section show that the multipath-to-direct signal ratio at the output of the array varies considerably as a function of multipath delay and reference synchronization error.

28

A very large value of this ratio -- occurring when the multipath com-
ponent is more closely synchronized with the reference than the direct
component -- is not necessarily indicative of poor performance, however,
since a portion of the specular multipath signal at the array output
is usable for data-detection purposes. The adaptive array acts as a
diversity receiver adjusting the gains of the two output components
according to their input amplitudes and relative synchronization with
the reference signal. A meaningful array performance measure, therefore,
should reflect the characteristics of this diversity by indicating the
proportion of total power at the array output which is useful in a
post-array demodulator. To this end, the ratio of usable signal
power to noise power at the array output in a bandwidth equal to the
spectral width of the data modulation is determined in this section.
Usable signal power is defined here as the power in the signal component
which is correlated with the reference signal. Noise power includes
the power in the uncorrelated signal component and the power in the
thermal noise components which falls within the data bandwidth.

As a first step in the calculation, we consider the hypothetical
processing operation on the array output signal indicated in Fig. 12.
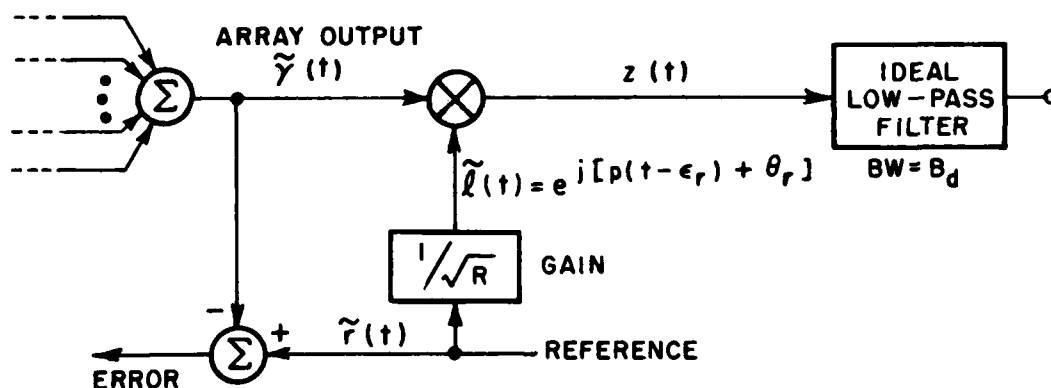
Fig. 12. Complex-envelope model of a
post-array demodulator.

The array output is multiplied by the reference signal and the product
is averaged in a low-pass filter whose bandwidth is matched to the
data rate. This operation is very similar analytically to coherent
detection of a coded communication signal. The essential difference
is that the multiplier reference signal in Fig. 12 contains both code
and data modulations whereas the derived reference in a coherent
detector contains only the code modulation. Thus, the filter output

29

in Fig. 12 is a d.c. level (ideally, in the absence of thermal noise, timing errors, and carrier frequency offsets) whereas the output of a coherent detector is the data modulation. Note that the thermal noise component at the array output and also at the multiplier output occupies the full spread bandwidth, B_{if}, of the received signal (see Eq. (17)). Hence, upon filtering to the data bandwidth, B_d, the power in this component is reduced by approximately the bandspreading ratio: B_{if}/B_d. The bandwidth of the uncorrelated signal component at the multiplier output is also approximately equal to B_{if}. It will be assumed that data filtering attenuates the power in this signal by the bandspreading ratio. With this approximation the signal-to-noise power ratio at the data filter output may be written as

$$(36) \qquad SNR_o = \frac{1}{\left(\dfrac{B_d}{B_{if}}\right)} SNR_y = \frac{E^2[y(t)]}{\left(\dfrac{B_d}{B_{if}}\right)(E[y^2(t)] - E^2[y(t)])}$$

where

$$(37) \qquad y(t) = \text{multiplier output process}$$
$$= \text{Re } z(t)$$

$$(38) \qquad z(t) = \tilde{\gamma}(t)\,\tilde{\ell}(t)^{+}$$

$$= \underline{w}(t)^{+}\left\{\tilde{\xi}_1(t)\underline{v}_1 + \tilde{\xi}_2(t)\underline{v}_2 + \tilde{\underline{n}}(t)\right\} e^{-j[p(t-\epsilon_r)+\theta_r]} \ .$$

$z(t)$ is the complex-valued, baseband process at the multiplier output associated with the complex envelope model of Fig. 12. Its real part, denoted above by $y(t)$, is the real signal at the multiplier output having physical significance:

$$(39) \qquad y(t) = \text{Re } z(t) = |\tilde{\gamma}(t)||\tilde{\ell}(t)| \cos[\underline{/\tilde{\gamma}(t)} - \underline{/\tilde{\ell}(t)}].$$

The asymptotic mean value of $z(t)$ is given by

$$(40) \qquad E[z(t)]\big|_{t\to\infty} = E\left[\tilde{\gamma}(t)\, e^{-j[p(t-\epsilon_r)+\theta_r]}\right]\bigg|_{t\to\infty}$$

$$= E[Q(t)]\big|_{t\to\infty} + E\left[\underline{w}(t)^{+}\underline{n}(t)\, e^{-j[p(t-\epsilon_r)+\theta_r]}\right]\bigg|_{t\to\infty}$$

$$= E[Q(t)]\big|_{t\to\infty} \ .$$

This result follows from Eqs. (38) and (28) upon noting that the thermal noise component in the multiplier output has zero mean value. Since the asymptotic mean value of z(t) was shown to be real-valued in the analysis following Eq. (28), it follows that the asymptotic mean value of y(t) is also given by Eq. (28), i.e.,

$$(41) \qquad E[y(t)]\big|_{t\to\infty} = \text{Re } E[z(t)]\big|_{t\to\infty} = E[z(t)]\big|_{t\to\infty}$$

where $\qquad E[z(\infty)] = $ a real number.

Therefore, the square of Eq. (28) gives the usable signal power in y(t):

$$(42) \qquad E^2[y(t)]\big|_{t\to\infty} = S|\underline{n}(\infty)^{\dagger}\underline{v}_1|^2 R_p^2(\epsilon_r) + M|\underline{n}(\infty)^{\dagger}\underline{v}_2|^2 R_p^2(\epsilon_r-\epsilon_m)$$

$$+ 2\sqrt{SM} \, R_p(\epsilon_r) \, R_p(\epsilon_r-\epsilon_m) \, \text{Re}\left\{ e^{j(\theta_1-\theta_2)} \right.$$

$$\left. \cdot (\underline{n}(\infty)^{\dagger}\underline{v}_1)(\underline{n}(\infty)^{\dagger}\underline{v}_2)^{\dagger} \right\} \quad .$$

The mean square value of y(t), i.e.,

$$(43) \qquad E[y^2(t)] = E[|z(t)|^2 - \{\text{Im } z(t)\}^2],$$

does not appear to be easily evaluated. An upper bound on the variance of y(t) in Eq. (36) may be obtained by neglecting the noise power contribution from the imaginary part of z(t):

$$E[|z(t)|^2 - E^2[y(t)] \geq \text{Var}[y(t)].$$

This upper bound is actually equal to the variance of the complex process z(t), in the limit as t→∞, since

$$(44) \qquad \text{Var}[z(t)] = E[|z(t) - E[z(t)]|^2]$$

$$= E[|z(t)|^2] - |E[z(t)]|^2$$

and the mean values of y(t) and z(t) are equal and real-valued in this limit from Eq. (41). Thus, a useful lower bound on the signal-to-noise ratio at the multiplier output is given by the signal-to-noise ratio in the complex signal z(t):

31

$$(45) \qquad SNR_z = \frac{|E[z(t)]|^2}{Var[z(t)]} \leq \frac{E^2[y(t)]}{Var[y(t)]} = SNR_y \quad .$$

The mean-square magnitude of $z(t)$ is equivalent to the total power present at the array output as seen from the expression

$$(46) \qquad E[|z(t)|^2] = E[|\tilde{y}(t)|^2 |\tilde{\ell}(t)|^2] = E[|\tilde{y}(t)|^2].$$

This quantity is calculated as follows:

$$(47) \qquad E[|\tilde{y}(t)|^2]\Big|_{t \to \infty} = E[|\underline{w}(t)^+ \tilde{\xi}_1(t)\underline{v}_1 + \tilde{\xi}_2(t)\underline{v}_2 + \tilde{\underline{n}}(t)|^2]\Big|_{t \to \infty}$$

$$\doteq S|\underline{n}(\infty)^+ \underline{v}_1|^2 + M|\underline{n}(\infty)^+ \underline{v}_2|^2$$

$$+ 2\sqrt{SM}\, R_p(\epsilon_m)\, Re\left\{ e^{j(\theta_1 - \theta_2)} \right.$$

$$\left. \cdot (\underline{n}(\infty)^+ \underline{v}_1)(\underline{n}(\infty)^+ \underline{v}_2)^+ \right\}$$

$$+ \sigma^2 |\underline{n}(\infty)|^2 \quad .$$

The variance of $z(t)$ follows as the difference in Eqs. (47) and (42). Upon combining the results in Eqs. (36)-(47), a lower bound is obtained for the signal-to-noise ratio at the filter output. This bound is

$$(48) \qquad SNR_0 \geq \frac{B_{if}}{B_d}\, SNR_z =$$

$$\left(\frac{B_{if}}{B_d}\right) \frac{\begin{array}{l} \frac{S}{\sigma^2}\left|\underline{n}(\infty)^+ \underline{v}_1\right|^2 R_p^2(\epsilon_r) + \frac{M}{\sigma^2}\left|\underline{n}(\infty)^+ \underline{v}_2\right|^2 R_p^2(\epsilon_r - \epsilon_m) \\[2mm] + 2\sqrt{\frac{S}{\sigma^2}\frac{M}{\sigma^2}}\, R_p(\epsilon_r)R_p(\epsilon_r - \epsilon_m)Re(X) \end{array}}{\begin{array}{l} \frac{S}{\sigma^2}\left|\underline{n}(\infty)^+ \underline{v}_1\right|^2 [1 - R_p^2(\epsilon_r)] + \frac{M}{\sigma^2}\left|\underline{n}(\infty)^+ \underline{v}_2\right|^2 [1 - R_p^2(\epsilon_r - \epsilon_m)] \\[2mm] + 2\sqrt{\frac{S}{\sigma^2}\frac{M}{\sigma^2}}\, [R_p(\epsilon_m) - R_p(\epsilon_r)R_p(\epsilon_m - \epsilon_r)]\, Re(X) \\[2mm] + |\underline{n}(\infty)|^2 \end{array}}$$

where
$$X = e^{j(\theta_1 - \theta_2)} (\underline{n}(\infty)^{\dagger} \underline{v}_1)(\underline{n}(\infty)^{\dagger} \underline{v}_2)^{\dagger} .$$

Note that the sum of the three numerator and four denominator terms in this bound is equal to the total power at the array output, Eq. (47), normalized by the element noise power, σ^2. In the absence of either multipath interference or reference timing error ($M = \epsilon_r = 0$), the bound in Eq. (48) reduces to the expected result for an array which is co-phased to the direct signal, i.e.,

$$(49) \qquad SNR_o \Big|_{\substack{M=0 \\ \epsilon_r=0}} = \frac{B_{if}}{B_d} \cdot \frac{\frac{S}{\sigma^2} \left| \underline{n}(\infty)^{\dagger} \underline{v}_1 \right|^2}{\left| \underline{n}(\infty) \right|^2} = \frac{B_{if}}{B_d} \left(\frac{mS}{\sigma^2} \right)$$

$$= \frac{B_{if}}{B_d} \left(\frac{mS}{N_o B_{if}} \right) = \frac{mS}{N_o B_d}$$

as verified using Eqs. (17), (23), and (24) where the mean weight vector is along the direct signal vector v_1:

$$\underline{n}(\infty) \Big|_{\substack{M=0 \\ \epsilon_r=0}} = \frac{\sqrt{R}\sqrt{S} \, \sigma^2}{\sigma^2 + mS} e^{j(\theta_1 - \theta_r)} \underline{v}_1 .$$

The ratio in Eq. (49) is independent of the bandspreading ratio whereas the signal-to-thermal noise ratios at array inputs and output decrease as the spread bandwidth, B_{if}, is increased.

The computer program in Appendix B was written to evaluate Eq. (48) for the case of a four-element linear array. The signal autocorrelation was assumed to be given by Eq. (15) and the bandspreading ratio was equated to the ratio of code and data rates, i.e.,

$$(50) \qquad \frac{B_{if}}{B_d} = \frac{\frac{1}{\Delta}}{\frac{1}{T_b}} = \frac{T_b}{\Delta} .$$

The signal-to-noise ratio at the data filter output with multipath absent, Eq. (49), was fixed at ten decibels. Figure 13 illustrates computed results for the same input power levels and angular separation as in Figs. 7 and 8. The two curves shown for each value of reference
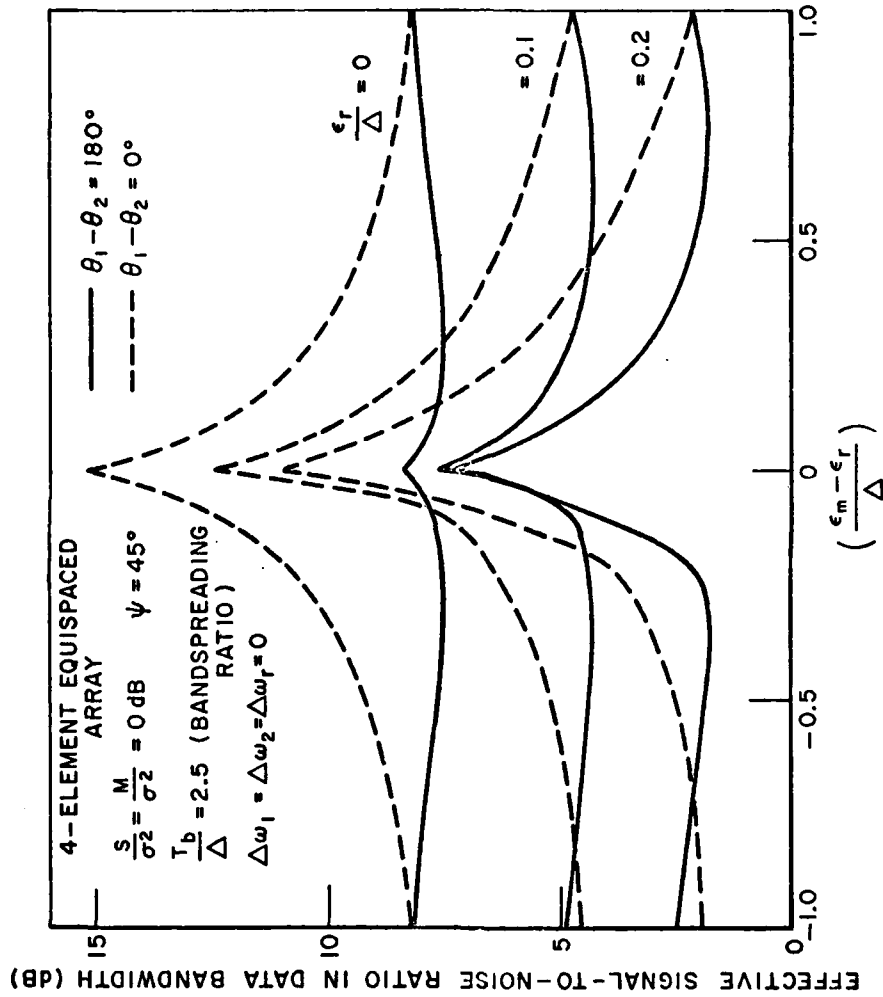
33

Fig. 13. Array output ratio of effective signal power-to-total noise power (in the information bandwidth).

timing error represent the upper and lower limits of data filter output signal-to-noise ratio (OSNR) versus carrier phase difference. As noted previously, the spread between these curves is an indication of the range over which the OSNR would vary periodically in time for very small differential doppler shift between input components. It is apparent in Fig. 13 that this spread is largest when both the input components are closely synchronized with the reference signal.

Consider the top pair of curves in Fig. 13 which correspond to perfect reference signal timing. In the absence of multipath, the OSNR would equal 10 dB; with perfectly-timed multipath present, the OSNR varies between 8.4 dB and 15.2 dB as the carrier phase difference varies between 180° and 0°. When the multipath signal is delayed by exactly one PN chip relative to direct and reference signals (i.e., an abscissa value of plus one), the OSNR is 8.2 dB and is independent of carrier phase difference. The loss of 1.8 dB relative to the multipath-absent case is the result of two effects. One, of course, is the increase in data filter output noise resulting from the presence of the uncorrelated multipath component. The other is due to a limitation in the spatial resolution capabilities of the array, i.e., the array cannot reject an uncorrelated interfering signal which is in close proximity ($\psi=45°$) to the desired signal without a loss in signal-to-thermal noise ratio at the array output. It can be shown from the results in Reference [13] that the loss due to this effect is equal to 1.3 dB for the input power ratios and angular separation of Fig. 13. In the absence of multipath, the array output signal-to-thermal noise ratio is equal to 6 dB; with equal-amplitude, uncorrelated multipath present, the direct signal-to-thermal noise ratio at the array output reduces to 4.7 dB. The uncorrelated multipath noise in the array output further reduces the effective signal-to-noise ratio to 4.2 dB, and the processing gain in the demodulator of 2.5 numeric (4.0 dB) increases the ratio to 8.2 dB at the filter output: the calculated value in Fig. 13.*

Consider now the lower pair of curves in Fig. 13 corresponding to a reference timing error of two-tenths of a PN chip relative to the direct signal. For uncorrelated multipath (i.e., an abscissa value of plus one), the OSNR is 2.1 dB which is 6.1 dB less than the value obtained above with zero reference timing error. This additional loss is partially accounted for by a reduction in correlated signal power in the array output in the amount

---

*The non-integer bandspreading ratio in Fig. 13 would not be implemented physically. This value was chosen for numerical convenience to obtain unity array input signal-to-thermal noise ratios in the program.

35

(51) $\quad R_p^2(\epsilon_r) = R_p^2(.2\Delta) = [(.8)(.92)]^2 = .542$

$$= -2.66 \text{ dB}.$$

The remainder is accounted for by the increase in noise contributed by the uncorrelated portion of the direct signal. That is, the direct signal-to-thermal noise ratio of 4.7 dB (3.0 numeric) with zero reference timing error is effectively reduced to

(52) $\quad \dfrac{3.0(.542)}{1+3.0(1-.542)} = .685 = -1.65 \text{ dB}$

when the timing error is two-tenths of a PN chip. The multipath "noise" in the array output further reduces this ratio to - 1.9 dB, and the 4.0 dB processing gain in the demodulator improves the ratio to the calculated value: 2.1 dB. In summary, the ideal OSNR of 10 dB with multipath absent is decreased by 7.9 dB when uncorrelated multipath is present of which 1.3 dB is accounted for by angular separation effects, 2.66 dB is due to correlated signal loss, and 3.94 dB is due to the increase in noise power. The significant observation to be made here is that the uncorrelated signal components at the array output are larger than the thermal noise components (compare the denominator terms in Eq. (52)). This condition is primarily the result of choosing a very small bandspreading ratio in Fig. 13. The bandspreading ratio was increased to a value of one-hundred in Fig. 14. With uncorrelated multipath present (abscissa value of plus one), the decrease in OSNR with reference timing error is considerably less than that in Fig. 13. That is, increasing the bandspreading ratio tends to raise the ends of the curves in Fig. 13. It is important to note here that increasing the code rate (for a fixed data rate) corresponds to decreasing the code bit duration, Δ. Thus, the improvement cited above -- which occurs when the reference timing error is maintained a fixed percentage of the code bit duration -- is realized only when reference timing error also decreases on an absolute time scale.

The values at the centers of the top pair of curves in Fig. 14 (where $\epsilon_r=0$) are the same as those in Fig. 13, i.e., the performance with perfectly synchronized signals is independent of the bandspreading ratio. As the reference timing error approaches a PN chip duration, the center values of the curves in Fig. 14 converge to a common value of OSNR: the same value as occurs when the timing error parameters are

$$\dfrac{\epsilon_r}{\Delta} = 0 \quad \text{and} \quad \dfrac{\epsilon_m - \epsilon_r}{\Delta} = +1.0.$$
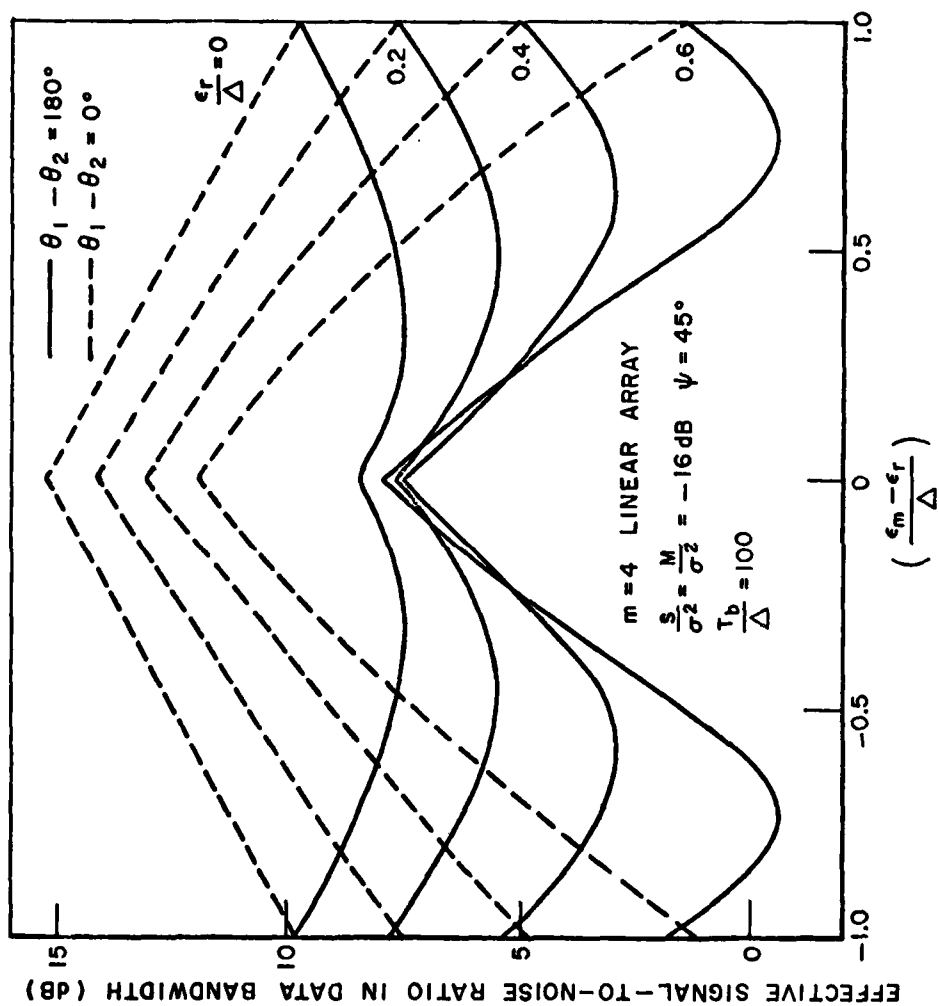
Fig. 14. Array output ratio of effective signal power-to-total noise power (in the information bandwidth).

37

This value is equal to 9.8 dB. Note the reversal of roles here; the perfectly-timed multipath component is the desired component while the direct component becomes uncorrelated with the reference as reference timing error increases to one PN chip. Also note that the center values of the dashed curves in Fig. 14 decrease monotonically toward 9.8 dB with reference timing error. In contrast, the center values of the solid curves first decrease slightly then increase toward 9.8 dB as reference timing error is increased. Similar behavior is noted for the center values of the curves in Fig. 13; these values converge to an OSNR of 8.2 dB as reference timing error approaches one PN chip.

The results in Fig. 15 show that performance improves when the angular separation between direct and multipath components is larger. The bandspreading ratio is equal to ten here and ψ has been increased to sixty degrees. For perfect reference signal timing ($\varepsilon_r=0$), the OSNR has a minimum value of 9.1 dB as the multipath delay and carrier phase difference parameters are varied.

The results in Fig. 16 illustrate performance behavior when the multipath signal is weaker than the direct signal. The parameters are the same as in Fig. 13 except for a 3 dB reduction in the multipath signal. The performance curves are nearly identical to those in Fig. 13 except for the center region which corresponds to the condition where the multipath signal is nearly aligned with the reference. The curves in Fig. 16 are depressed in this region relative to those in Fig. 13. This behavior reflects the lesser utility of the multipath signal for data demodulation purposes when its power is decreased relative to thermal noise power.

The results in Figs. 13-16 represent a partial description of array performance in a multipath envirnonment. Certain trends in basic behavior are apparent in these results. An important question at this point is the following: What design restrictions must be imposed on bandspreading ratio, reference timing error, and input angular separation to insure that worst-case performance is acceptable regardless of the multipath signal amplitude, delay, or carrier phase angle? If acceptable performance is represented, for example, by a decrease in the OSNR ratio of no more than one decibel from its ideal value of 10 dB for no more than fifty percent of the time, what restrictions must be imposed? A complete answer to this question must take into account other effects besides those studied here; however, the results in Figs. 13-16 indicate that the inequalities

$$\psi \quad > \quad 60°$$

$$\frac{T_b}{\Delta} \quad > \quad 100$$

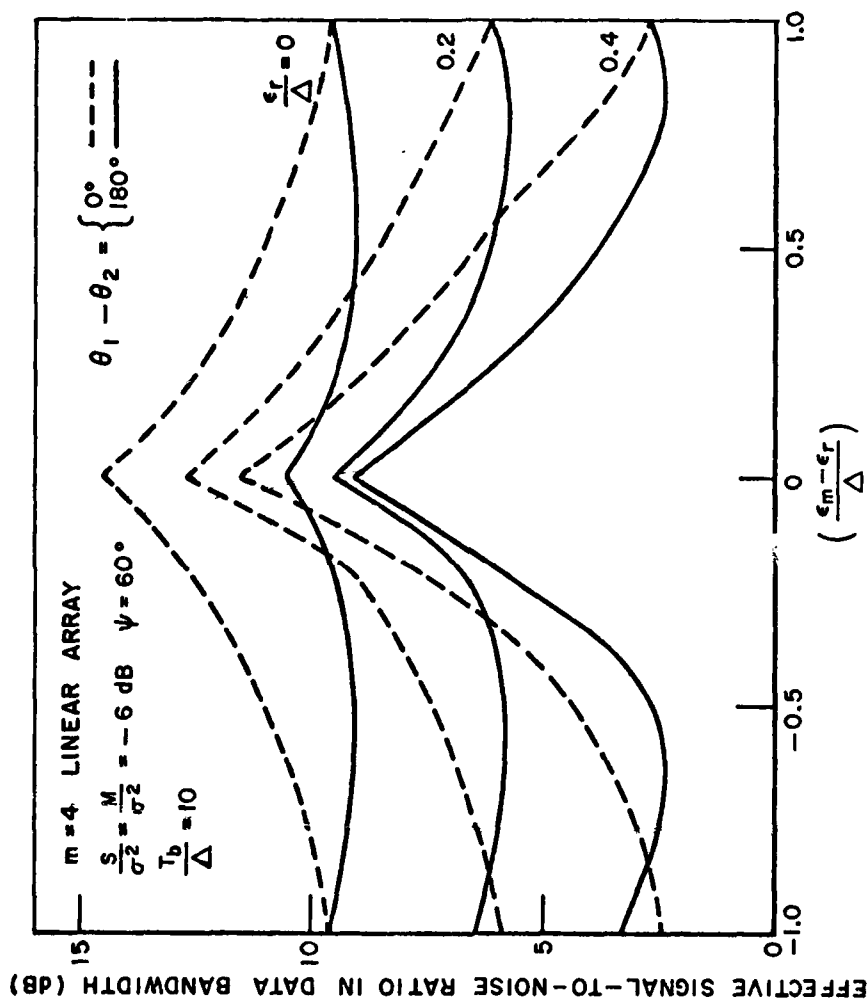$$\varepsilon_r \quad < \quad 0.05\Delta$$

Fig. 15. Array output ratio of effective signal power-to-total noise power (in the information bandwidth).
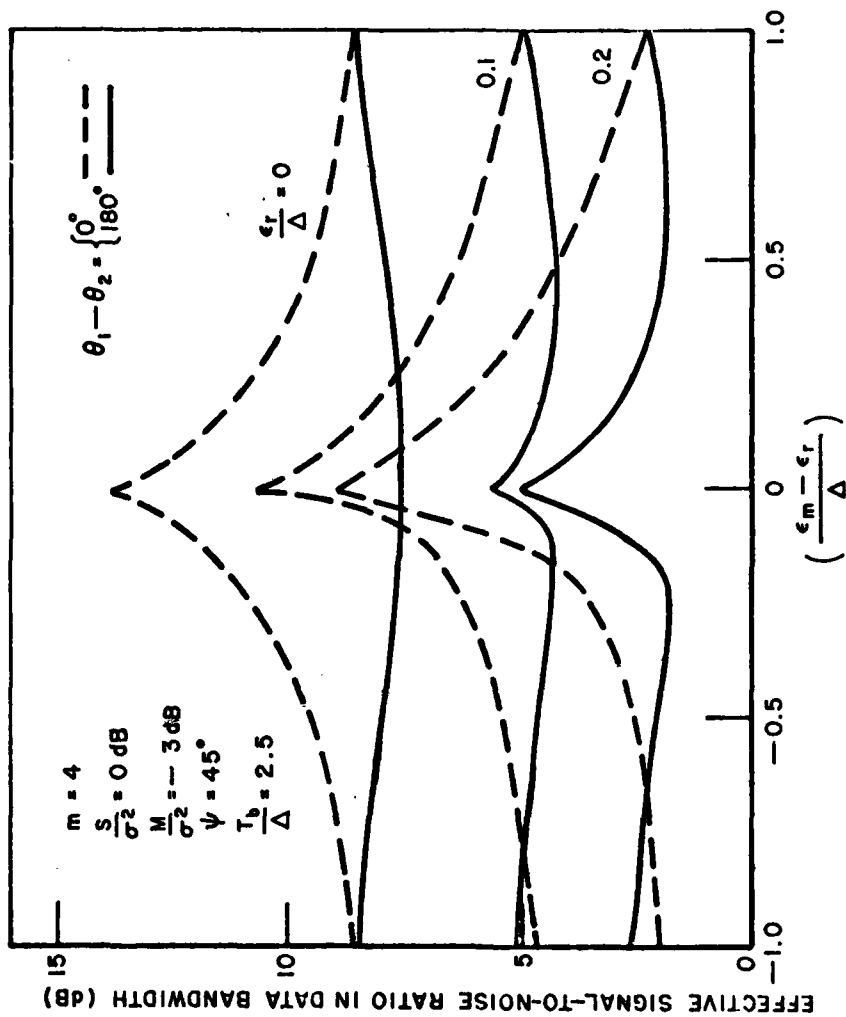
39

Fig. 16. Array output ratio of effective signal power-to-total noise power (in the information bandwidth).

would most likely need to be satisfied as minimum requirements. The shape of the performance curves might also vary somewhat as a function of array geometry and number of array elements. Additional computer evaluations are needed to resolve these questions. Additional analyses are also needed to determine the multipath response characteristics of delay-lock loop tracking receivers[14]. These receivers are used to estimate code timing ($\hat{\epsilon}_r$) from the array output signal in practical implementations. For many applications, the locked local code in the delay-lock receiver is used in generating the reference signal for the array. The results of this study indicating the timing error characteristics of the locked local code versus input parameters should then be merged with results similar to those in Figs. 13-16 to determine steady-state operating characteristics of the composite system. A final refinement should also include an investigation of the characteristics of processed-reference signals, i.e., of "bootstrap" reference-generation loops, with multipath of arbitrary differential doppler shift.

IV. CONCLUSIONS

The steady-state response of an adaptive antenna array to a received signal which contains a specular multipath component has been examined. It was found that closed-form solutions for the response could be obtained when the difference in carrier frequencies of the direct and reflected components was small and the carrier frequency offset of the array reference signal was negligible. The results show that the array acts like a diversity receiver which weights the input components in accordance with their relative correlation with the array reference signal. This correlation depends on the time-delay of the input components relative to the time-base of the reference signal and on the structure and bandwidth of modulation contained in these signals.

It is shown that the array adjusts the amplitudes and carrier phases of the output signal components in such a manner that the carrier phase of their resultant sum is aligned on the average with the carrier phase of the array reference signal.

The results also show that not all of the power in the output signal components is usable for data demodulation purposes as a consequence of delay differences in their modulations. The ratio of usable signal power to unusable signal power plus thermal noise power at the output of a coherent detector is calculated. The detector bandwidth is matched to the data rate, and its reference signal is matched in delay and carrier phase to the array reference signal. Numerical evaluations of this performance ratio are presented for the case of a four-element linear array where the desired input signal is

41

a bi-phase modulated, pseudonoise-coded, communication signal. These
results show that ideal performance is obtained when the multipath
component is absent and the array reference signal is perfectly
synchronized with the direct component. Performance degrades when
multipath is present and the reference signal is imperfectly aligned
with either input component. The amount of degradation is dependent
on several parameters. It is found that worst-case performance with
respect to the relative carrier phases of the input components occurs
when the carrier phase difference (at the array phase center) is equal
to 180°. It is also shown that increasing the bandspreading ratio,
i.e., the ratio of code-to-data rates, lessens the performance degra-
dation provided the timing error of the direct component is maintained
at a very small fraction of the pseudonoise code bit duration. The
performance degradation is also less severe when the angular separation
of input components is increased. In general, the angular separation
must exceed one-half the (natural) half-power beamwidth of the
(co-phased) array to avoid significant degradation for arbitrary
amplitude, delay, and carrier phase of the multipath component.

REFERENCES

1. Widrow, B., P.E. Mantey, L.J. Griffiths, and B.B. Goode,
    "Adaptive Antenna Systems," Proc. IEEE, 55 12 (December 1967),
    pp. 2143-2159.

2. Shor, S.W.W., "Adaptive Technique to Discriminate Against
    Coherent Noise in a Narrow-band System," J. Acoust. Soc. Am.,
    39 (January 1966), pp. 74-78.

3. Applebaum, S.P., "Adaptive Arrays," Special Projects Laboratory
    Report SPL-TR66-1, August 1966, Syracuse University Research
    Corporation, Syracuse, N.Y.

4. Baird, C.A. and C.L. Zahm, "Performance Criteria for Narrowband
    Array Processing," 1971 IEEE Conference on Decision and Control,
    Miami Beach, Florida, December 15-17, 1971.

5. Baird, C.A., Jr., G.P. Martin, G.G. Rassweiler, and C.L. Zahm,
    "Adaptive Processing for Antenna Arrays," Final Report, Radiation
    Systems Division, Melbourne, Florida, June 1972.

6. Riegler, R.L. and R.T. Compton, Jr., "An Adaptive Array for
    Interference Rejection," Proc. IEEE, 61, 6 (June 1973), p. 748.

7. Compton, R.T., Jr., "Adaptive Antenna Arrays for Aircraft
    Communication Systems, Report 3098-2, January 1972, The Ohio
    State University ElectroScience Laboratory, Department of Electrical
    Engineering; prepared under Contract N00014-67-A-0232-0009 for
    Office of Naval Research, Arlington, Va.

8. Brennan, L.E. and I.S. Reed, Theory of Adaptive Radar, Project
    Memorandum 073-1, Technology Service Corporation, Santa Monica,
    California, June 1971.

9. Berni, A.J., "Angle of Arrival Estimation Using an Adaptive
    Array," Report 3435 1, June 1973, The Ohio State University
    ElectroScience Laboratory, Department of Electrical Engineering;
    prepared under Contract DAAG39-72-C-0169 for Department of the
    Army, Harry Diamond Laboratories.

10. Reinhard, K.L., "Adaptive Array Techniques for TDMA Network
    Protection," Section II of R.J. Huff, "Coherent Multiplexing
    and Array Techniques," Report 2738-3, 9 February 1971, The Ohio
    State University ElectroScience Laboratory, Department of
    Electrical Engineering; prepared under Contract F30602-69-C-0012
    for Rome Air Development Center, Griffiss Air Force Base, New
    York.

43

11. Reinhard, K.L., "An Adaptive Array for Interference Rejection in a Coded Communication System," Report 2738-6, April 1972, The Ohio State University ElectroScience Laboratory, Department of Electrical Engineering; prepared under Contract F30602-69-C-0112 for Rome Air Development Center, Griffiss Air Force Base, New York.

12. Huff, R.J. and K.L. Reinhard, "Coherent Multiplexing and Array Techniques," Report 2738-9, June 1972, The Ohio State University ElectroScience Laboratory, Department of Electrical Engineering; prepared under Contract F30602-69-C-0112 for Rome Air Development Center, Griffiss Air Force Base, New York.

13. Reinhard, K.L., "Adaptive Antenna Arrays for Coded Communication Systems," Report 3364-2, November 1974, The Ohio State University ElectroScience Laboratory, Department of Electrical Engineering; prepared under Contract F30602-72-C-0162 for Rome Air Development Center, Griffiss Air Force Base, New York. (In preparation). Also Ph.D. Dissertation.

14. Schwegman, W.C. and R.T. Compton, Jr., "An Experimental, Spread Spectrum Adaptive Array," Report 3098-4, January 1974, The Ohio State University ElectroScience Laboratory, Department of Electrical Engineering; prepared under Contract N00014-67-A-0009 for Office of Naval Research.

15. Swarner, W.G. and A.J. Berni, Final Report 3435-2, The Ohio State University ElectroScience Laboratory, Department of Electrical Engineering; prepared under Contract DAAG39-72-C-0169 for Department of the Army, Harry Diamond Laboratories, (In preparation).

44

APPENDIX A
COMPUTER PROGRAM I


```
1,/P
  1    C   HP 2115A   COMPUTER BASIC LANGUAGE PROGRAM
  2    C       MULTIPATH-TO-DIRECT SIGNAL RATIO
  3    C   M=NUMBER OF ARRAY ELEMENTS
  4    C   S1=INPUT SIGNAL TO NOISE RATIO
  5    C   M1=INPUT MULTIPATH TO NOISE RATIO
  6    C   PS1=ANGULAR SEPARATION (DEGREES)
  7    C   E1=REFERENCE TIMING ERROR
  8    C   E2=MULTIPATH TIMING ERROR
  9    C   T=CARRIER PHASE DIFFERENCE (DEGREES)
 10    C   R=ARRAY OUTPUT RATIO
 11    10 PRINT "M,S1,M1,PS1=";
 12    20 INPUT M,S1,M1,P
 13    30 PRINT
 14    40 PRINT
 15    60 FOR E1=0 TO .9 STEP .1
 16    70 FOR E2=.8 TO -.8 STEP -.2
 17    75 FOR T=0 TO 180 STEP 30
 18    80 LET P2=3.14159*P/180
 19    85 LET T2=3.14159*T/180
 20    90 LET V=SIN(M*P2/2)/(M*SIN(P2/2))
 21   100 LET V1=1-V*V
 22   110 LET Q1=1-ABS(E1)
 23   120 LET Q2=1-ABS(E2)
 24   130 LET Q3=1-ABS(E2-E1)
 25   140 IF Q3>1.00000E-03 THEN 160
 26   150 LET Q3=0
 27   160 LET Q=Q3/Q1
 28   170 LET W=SQR(M1/S1)
 29   175 LET NO=Q*W*(1+M*S1*V1)-M*W*S1*Q2*V1
 30   180 LET N=(V+NO*COS(T2))*(V+NO*COS(T2))+(NO*SIN(T2))*(NO*SIN(T2))
 31   185 LET DO=Q*W*V
 32   186 LET D1=1+M*M1*V1*(1-Q*Q2)
 33   190 LET D=(D1+DO*COS(T2))**2+(DO*SIN(T2))**2
 34   220 LET R=4.34295*LOG(M1*N/(S1*D))
 35   230 PRINT E1,E2,T,R
 36   240 NEXT T
 37   250 PRINT
 38   260 NEXT E2
 39   270 PRINT
 40   280 NEXT E1
 41   300 END
```

45

APPENDIX B
COMPUTER PROGRAM II

```
1          DIMENSION L(7),RDB(7)
2          COMPLEX CDELTH,A,B,CV12,WV1,WV2,WCR,CSXM
3          COMMON ER,EM,ED,CR,CM,CD,BSR
4          ANUM=4.0
5          BSR=2.5
6          PSID=45.0
7          OSNRM=10.0
8          SMRI=1.0
9          PSI=3.1415926*PSID/180.0
10         V12=SIN(ANUM*PSI/2.0)/(ANUM*SIN(PSI/2.0))
11         CV12=CMPLX(V12,0.0)
12         RSN=OSNRM/(ANUM*BSR)
13         RMN=RSN/SMRI
14         WRITE(6,10)ANUM,BSR,PSID,OSNRM,SMRI,RSN,RMN
15      10 FORMAT(5HANUM=,E10.4,/,4HBSR=,E10.4,/,4HPSI=,E10.4,/,6HOSNRM=,
16         CE10.4,/,4HSMR=,E10.4,/,4HRSN=,E10.4,/,4HRMN=,E10.4,////)
17         DO 90 I=1,10
18         FI=I
19         FR=(FI-1.0)/10.0
20         WRITE(6,20)ER
21      20 FORMAT(///,3HER=,F4.1)
22         DO 30 M=1,7
23      30 L(M)=30*(M-1)
24         WRITE(6,40)(L(N),N=1,7)
25      40 FORMAT(12HDELTA-THETA=,2X,7(I4,10X),/,3HEM=,/)
26         DO 90 J=1,21
27         FJ=J
28         EM=(FI+FJ-12.0)/10.0
29         ED=EM-ER
30         CR=CORR(ER)
31         CM=CORR(EM)
32         CD=CORR(ED)
33         DO 60 K=1,7
34         FK=K
35         DELTHD=(FK-1.0)*30.0
36         DELTH=3.1415926*DELTHD/180.0
37         CDELTH=CMPLX(COS(DELTH),SIN(DELTH))
38         AA=CR*(1.0+ANUM*RMN)-CM*CD*ANUM*RMN
39         A1=AA*SQRT(RSN)
40         A2=ANUM*RSN*SQRT(RMN)*V12*(CR*CM-CD)
41         BB=CD*(1.0+ANUM*RSN)-CM*CR*ANUM*RSN
42         B2=BB*SQRT(RMN)
43         B1=ANUM*RMN*SQRT(RSN)*V12*(CM*CD-CR)
44         ARL=A1*COS(DELTH)+A2
45         AIM=A1*SIN(DELTH)
```

46

```
46          BRL=B1*COS(DELTH)+B2
47          BIM=B1*SIN(DELTH)
48          A=CMPLX(ARL,AIM)
49          B=CMPLX(BRL,BIM)
50          WV1=CONJG(A+CV12*B)
51          WV2=CONJG(CV12*A+B)
52          WCR=CV12*A*CONJG(B)
53          ZA=CABS(A)
54          ZB=CABS(B)
55          ZW1=CABS(WV1)
56          ZW2=CABS(WV2)
57          ZWW=(ZA*ZA+ZB*ZB+2.0*REAL(WCR))/ANUM
58          CSXM=CDELTH*WV1*CONJG(WV2)
59          SXM=REAL(CSXM)
60          PS=RSN*ZW1*ZW1*CR*CR+RMN*ZW2*ZW2*CD*CD
61          PS=PS+SQRT(RSN)*SQRT(RMN)*CR*CD*2.0*SXM
62          PN=RSN*ZW1*ZW1*(1.0-CR*CR)+RMN*ZW2*ZW2*(1.0-CD*CD)
63          PN=PN+SQRT(RSN)*SQRT(RMN)*(CM-CR*CD)*2.0*SXM+ZWW
64          RATIO=BSR*PS/PN
65          RDB(K)=10.0*ALOG10(RATIO)
66       60 CONTINUE
67          WRITE(6,70)EM,(RDB(M),M=1,7)
68       70 FORMAT(5X,F4.1,5X,10(F6.2,8X))
69       90 CONTINUE
70          STOP
71          END
72          FUNCTION CORR(X)
73          COMMON ER,EM,ED,CR,CM,CD,BSR
74          AX=ABS(X)
75          IF(1.0-AX)25,25,35
76       25 CORR=0.0
77          GO TO 55
78       35 CORR=(1.0-AX/BSR)*(1.0-AX)
79       55 RETURN
80          END
81          FIN$
```

47

DOCUMENT CONTROL DATA - R & D

(Security classification of title, body of abstract and indexing annotation must be entered when the overall report is classified)

1. ORIGINATING ACTIVITY *(Corporate author)*	2a. REPORT SECURITY CLASSIFICATION
ElectroScience Laboratory Department of Electrical Engineering, The Ohio State University, Columbus, Ohio 43212	Unclassified
	2b. GROUP

3. REPORT TITLE

ADAPTIVE ARRAY PERFORMANCE WITH SPECULAR MULTIPATH

4. DESCRIPTIVE NOTES *(Type of report and inclusive dates)*
Quarterly Technical Report - March 1, 1973 to June 1, 1973

5. AUTHOR(S) *(First name, middle initial, last name)*

Reinhard, K. L.

6. REPORT DATE	7a. TOTAL NO. OF PAGES	7b. NO. OF REFS
February 1974	47	13

8a. CONTRACT OR GRANT NO.	9a. ORIGINATOR'S REPORT NUMBER(S)
N00019-73-C-0195	
b. PROJECT NO.	ElectroScience Laboratory 3576-2
c.	9b. OTHER REPORT NO(S) *(Any other numbers that may be assigned this report)*
d.	

10. DISTRIBUTION STATEMENT

DISTRIBUTION STATEMENT A

Approved for public release;
Distribution Unlimited

11. SUPPLEMENTARY NOTES	12. SPONSORING MILITARY ACTIVITY
	Department of the Navy Naval Air Systems Command Washington, D.C. 20360

13. ABSTRACT

    This report describes the theoretical performance of an adaptive antenna array in a multipath signal environment. The array response to a coded communication signal comprised of a direct (line-of-sight) component and a specular multipath component is determined for the case in which differential doppler frequency shift between components is negligible compared to the reciprocal time constants of the array processing loops.

    Performance analyses are presented which determine the ratio of powers in the direct and multipath signal components at the array output. The fraction of total power at the array output which is usable or beneficial for post-array data demodulation is also calculated. Computer evaluations are presented which illustrate the dependence of these ratios on received signal amplitudes, carrier phases, angle-of-arrival separation, and relative synchronization with a coded reference signal which is locally generated at the receiving array.

DD FORM 1473
I NOV 65

14 KEY WORDS	LINK A		LINK B		LINK C	
	ROLE	WT	ROLE	WT	ROLE	WT
Antennas						
Adaptive arrays						
Multipath interference						
Coded communication signals						
Analytical performance						
Computer evaluations						

END

DATE
FILMED

3-83

DTIC